THE ASTROPHYSICAL JOURNAL, 331:876–897, 1988 August 15

THE PRESENCE OF HELIUM IN HOT DA WHITE DWARFS: THE ROLE OF RADIATIVE LEVITATION AND THE CASE FOR STRATIFIED ATMOSPHERES

S. VENNES, C. PELLETIER, G. FONTAINE,[1] AND F. WESEMAEL
Département de Physique, Université de Montréal
Received 1987 October 1; accepted 1988 February 10

ABSTRACT

The role of helium radiative levitation in the envelopes of hot DA white dwarfs is investigated. This is motivated by the presence of photospheric traces of helium inferred from short-wavelength observations of several hot DA white dwarfs or measured from optical observations of even hotter DAO stars. Using a simple prescription for the computation of the radiative acceleration, explicit time-dependent calculations of helium diffusion in presence of radiative support are carried out in evolving DA models. These computations firmly establish that the helium distribution in the outermost layers of the models relaxes extremely rapidly to a configuration corresponding to diffusive equilibrium. Thus, the regions accessible to direct observation show only equilibrium helium abundances and are totally decoupled from the evolving internal helium profile. This welcome decoupling permits to determine more quantitatively the equilibrium abundances of helium in these regions with the help of inexpensive static envelope models. To this end, detailed calculations of the selective acceleration on helium embedded in a hydrogen plasma are carried out for a wide range of physical conditions. It is shown that the abundances of helium supported by radiative forces in the atmospheric layers of hot DA white dwarfs are too small by at least two orders of magnitude to account for the observations. Hence, a more efficient mechanism than radiative levitation must be invoked to compete against gravitational settling in these stars. A number of mechanisms are discussed, and it is suggested that an equilibrium between ordinary diffusion (driven by a composition gradient) and settling may be a most attractive possibility. In this model, hot DA white dwarfs can be interpreted as stratified objects with an outer layer of hydrogen which is sufficiently thick that radiation in the visible escapes only from hydrogen-rich regions, and yet sufficiently thin that the EUV/soft X-ray radiation escapes from deeper layers, polluted by the tail of the helium equilibrium distribution which extends upward. A simple opacity effect leads naturally to a positive correlation between helium abundance and effective temperature: as cooling proceeds, the opacity of the atmospheric layers increases and the EUV/soft X-ray photosphere recedes to the surface, to regions of smaller helium abundance. However, the observed correlation is steeper than that obtained for an evolving model in which the mass of the outer layer of hydrogen is kept constant. The observations can be accounted for if the mass and thickness of the hydrogen layer increase with decreasing effective temperature. For example, a value $\mathrm{He/H} = 10^{-2.5}$ (which is typical of DAO stars) is present at the soft X-ray photosphere of a stratified 60,000 K, 0.6 $M_\odot$ DA model if the hydrogen layer contains only a fractional mass $\sim 10^{-14.7}$. To account for the observed value $\mathrm{He/H} \sim 10^{-5}$ (more typical of $\sim$30,000 K DA stars), the model requires a hydrogen layer containing a fractional mass $\sim 10^{-13.3}$. These numbers imply that hydrogen-helium separation still goes on in hot DA white dwarfs and argue against the existence of strong winds and substantial residual burning in such stars. The suggestion that hot DA white dwarfs have thin hydrogen-rich layers further adds to mounting evidence in favor of thin hydrogen and helium layers in white dwarfs in general. This is in strong contradiction with the predictions of standard evolution theory.

Subject headings: diffusion — stars: abundances — stars: atmospheres — stars: white dwarfs

I. INTRODUCTION

Over the last decade, observations of white dwarfs at increasingly higher sensitivity and through various spectral windows have revealed a wealth of information about trace element constituents in their atmospheres. The presence of trace species in an otherwise chemically pure environment (either H or He) indicates that element settling does not go totally unimpeded in a white dwarf star. And, indeed, it has long been known (Schatzman 1958) that, *in the absence of competing mechanisms*, heavy elements settle extremely rapidly below the photosphere in such a star. The more recent estimates of diffusion time scales in white dwarfs (e.g., Fontaine and Michaud 1979; Vauclair, Vauclair, and Greenstein 1979; Alcock and Illarionov 1980; Muchmore 1984; Paquette *et al.* 1986*a*) verify this basic conclusion and confirm the need for mechanisms competing against settling. Among a number of possibilities, it is generally believed that processes such as radiative levitation, ordinary diffusion, convective dilution, accretion, and stellar winds can, under appropriate circumstances, partially counterbalance the effects of gravitational settling in white dwarfs. At the present time, the absolute and relative efficiencies of these mechanisms as well as their intricate interactions are far from being understood. Likewise, the complex interplay of such processes with evolutionary effects is not well known and deserves further study. Ultimately, one can hope to formulate a consistent theory of the spectral evolution of white dwarf stars. As part of this long-range endeavor, we

[1] E.W.R. Steacie Memorial Fellow.

examine here the problem of diffusion in presence of radiative forces as well as the effects of ordinary diffusion as possibilities for explaining the presence of traces of helium in the atmospheres of hot, H-rich (DA) white dwarfs.

Considerable attention has been given recently to the use of short-wavelength observations to probe the structure of white dwarf atmospheres (see Holberg 1987*a* for an excellent review of these developments). A fundamental result has been the early realization by Shipman (1976) that the helium- and metal-deficient atmosphere of a sufficiently hot ($T_e \gtrsim 30{,}000$ K) DA white dwarf would offer a minimal opacity to soft X-ray radiation allowing such photons to escape in large numbers from relatively deep ($\tau \gtrsim 60$) layers. This attractive suggestion was initially used to account for the then surprisingly large EUV/soft X-ray emission observed from objects such as Sirius B, and, later, from HZ 43 and Feige 24. Since then, the thermal model has been invoked in the analyses of several hot, DA white dwarfs, all observed from the *Einstein* or the *EXOSAT* satellite, or from both. The individual analyses are discussed in detail in Kahn *et al.* (1984), Holberg, Wesemael, and Hubený (1984), Heise (1985), Petre, Shipman, and Canizares (1986), Paerels *et al.* (1986*a*, *b*, 1987, 1988), Jensen *et al.* (1986), Pravdo *et al.* (1986), Jordan *et al.* (1987), Petre and Shipman (1987), Paerels and Heise (1988), and Heise *et al.* (1988).

One interesting property of the thermal model is that the EUV/soft X-ray flux is very sensitive to opacity sources provided by trace amounts of helium and heavier elements that may be present in the atmosphere. Quite naturally, this property has been extensively used by various modelers to *infer* the presence of trace absorbers heavier than hydrogen. In particular, helium abundances ranging from He/H $\sim 10^{-2.3}$ to less than $\sim 10^{-5.3}$ have been derived from EUV/soft X-ray observations of several hot DA white dwarfs found in the range $24{,}500 \lesssim T_e \lesssim 62{,}000$ K. It seems important to remind the reader that, for reasons of simplicity, it has been assumed that *only* helium provides the required opacity source in the various analyses, so that only helium abundances are inferred. In addition, it has been assumed that helium is *uniformly* distributed in the atmosphere. Because of these limitations, Kahn *et al.* (1984) clearly acknowledge that their inferred He abundances must be considered with due caution. For example, they mention that helium remains the dominant opacity source below 227 Å only if the abundances of heavier elements can be maintained below 10^{-3} of their solar values. Similar remarks have also been made by Petre, Shipman, and Canizares (1986), Jordan *et al.* (1987), and Paerels and Heise (1988).

There exists another subgroup of hot, H-rich white dwarfs for which atmosphereic traces of helium have been derived. By contrast with the objects we have been discussing, helium is *spectroscopically visible* in the so-called DAO white dwarfs, and the derived abundances rest correspondingly on much firmer grounds. The analysis of Wesemael, Green, and Liebert (1985) suggests that the DAO stars are characterized by $50{,}000 \lesssim T_e \lesssim 70{,}000$ K and He/H $\sim 10^{-2.0}$ (see also earlier relevant results by Koester, Liebert, and Hege 1979; Mendez *et al.* 1981). These stars are thus generally hotter and more He-rich than the DA objects observed so far at shcrt wavelengths.

In order to explain the traces of helium inferred or measured in the atmospheres of hot DA/DAO objects, one must find a mechanism that can compete against gravitational settling in these stars. A very popular process—and perhaps the most natural mechanism that comes to mind—is the idea that the relatively large radiative fluxes found in the objects of interest can support finite amounts of helium against settling through, mostly, bound-bound transitions (Kahn *et al.* 1984). This seems attractive because, for example, we know from the work of Vauclair, Vaulair, and Greenstein (1979) that radiative support on heavier elements, such as C, N, and O, is possible in hot white dwarfs. In addition, one would expect a correlation between the helium abundance and the effective temperature in the sense that larger quantities of helium should be supported in hotter stars because their radiative fluxes are larger. Such a correlation, first pointed out by Petre, Shipman, and Canizares (1986), is definitely suggested by the analyses of hot DA white dwarfs (see below).

Motivated by these arguments, we first investigate in this paper the role of helium levitation in the atmospheres of hot DA white dwarfs. Although this mechanism has been called upon by a large number of authors, the present effort is, to our knowledge, the first systematic and quantitative study that has been attempted. As such, we devote § II to a discussion of the general problem of diffusion in presence of radiative forces. We carry out exploratory time-dependent calculations of He diffusion in DA models using a simplified prescription for the computation of the radiative acceleration on He. These calculations show that the helium distribution in the regions of the envelope directly accessible to observations relaxes extremely rapidly to its equilibrium configuration. In § III, we take advantage of these results and compute detailed photospheric equilibrium He abundances in static envelope models of DA white dwarfs. These computations make use of the extensive grid of He radiative forces in a H plasma developed recently by Vennes (1985). The abundances of He supported by radiative forces are found to be too small to account for the observations. In the next section, we then briefly discuss a number of alternate possibilities and develop fully the idea that DA white dwarfs have a very thin outer layer of hydrogen to the extent that helium can pollute the EUV/soft X-ray photosphere and provide the required opacity. The implications of this model invoking an equilibrium between gravitational settling and ordinary diffusion are also discussed. We summarize our findings in the last section. Preliminary results of the present investigation have been presented by Vennes *et al.* (1987) and Fontaine *et al.* (1987).

II. DIFFUSION IN PRESENCE OF RADIATIVE FORCES

a) Diffusion Equation and Equilibrium

We consider the problem of H–He chemical separation in presence of radiative forces in evolving white dwarfs. To this end, we follow closely the method presented by Pelletier *et al.* (1986). Although details can be found in that reference, it is worth recalling briefly that the effects of diffusion on the structure of white dwarf envelope models and the feedback effects of the structure on diffusion are consistently taken into account along evolutionary tracks provided by the calculations of Winget, Lamb, and Van Horn (1988). The envelope models, with variable chemical composition as imposed by diffusion, use the input physics of Fontaine and Van Horn (1976) augmented by the equation of state tables of Fontaine, Graboske, and Van Horn (1977) and the newer radiative opacities for the Iben I ($X = 0.999$) and Iben V ($Y = 0.999$) compositions provided by Huebner (1980). The situation is

idealized by considering a two-component model, which necessitates the integration of only one diffusion equation and simplifies considerably the problem. In the present case, we consider a stellar plasma made of two ionic constituents of average charge Z_1 (hydrogen) and Z_2 (helium). For a H–He mixture of arbitrary proportions, the relative diffusion velocity of helium with respect to hydrogen can be written,

$$w_{12} = D_{12}(1+\gamma)\left[-\frac{\partial \ln c_2}{\partial r} + \left(\frac{A_1 Z_2 - A_2 Z_1}{Z_1 + \gamma Z_2}\right)\frac{m_p g}{kT} + \left(\frac{Z_2 - Z_1}{Z_1 + \gamma Z_2}\right)\frac{\partial \ln p_i}{\partial r} + \left(\frac{A_1 A_2}{A_1 + \gamma A_2}\right)\frac{m_p g_r}{kT}\right], \quad (1)$$

where D_{12} is the diffusion coefficient, $\gamma \equiv n_2/n_1$ is the helium-to-hydrogen number density ratio, $c_2 \equiv n_2/(n_1 + n_2)$, r is the radial coordinate, $Z_i(A_i)$ is the average charge (atomic weight) of ions of species i (= 1, 2), m_p is the proton mass, g is the local gravity, k is Boltzmann's constant, T is the temperature, $p_i = p_1 + p_2$ is the ionic pressure, and g_r is the upward *selective* radiative acceleration exerted on helium in the plasma. The sign convention is such that if w_{12} is negative, helium sinks into the star with respect to hydrogen. This diffusion equation is the same as that derived by Pelletier *et al.* (1986; their eq. [5]) augmented with a term which corresponds to the additional process considered in this paper namely radiative forces (see Chapman and Cowling 1970). It ignores thermal diffusion which can be safely neglected in white dwarf plasmas according to Paquette *et al.* (1986*a*).

In general, in the absence of sources or sinks of matter, a system undergoing diffusion processes evolves toward an equilibrium state in which $w_{12} = 0$ everywhere. In the present case, the second and third terms[2] in the diffusion equation are always negative and, thus, induce helium to sink into the star. Equilibrium can be reached through restoring forces provided by the concentration gradient term (if a sufficiently large negative buildup of helium is achieved) and the radiative acceleration term (which is always positive). Note that this last term can only be important if helium is trace ($\gamma \ll 1$), and if the layers under consideration are near the photosphere (through the approximate relation $g_r \propto T_e^4/T$, as derived, for example, by Michaud *et al.* 1976). In deeper shells in a star, the radiative acceleration term always becomes smaller than the gravitational settling term, and no diffusive equilibrium due to radiative levitation is possible there. At best, radiative forces can slow down the settling of heavy elements in such a case, but, in practice, their effects become utterly negligible. We note, after Paquette *et al.* (1986*a*), that radiative support on heavy elements can only be expected to play a significant role in the outermost layers of H-rich white dwarfs hotter than $T_e \sim 20{,}000$ K.

The method adopted here and in Pelletier *et al.* (1986) takes fully into account the effects of finite abundances and the effects of evolution on the distributions of the diffusing elements. This is to be contrasted with the method used in Paquette *et al.* (1986*a*) (and numerous similar studies) in which *e*-folding diffusion time scales are estimated by neglecting the concentration gradient term in the diffusion equation and assuming negligible abundances. Under these assumptions, the latter method becomes essentially local in nature. And, indeed, one then computes diffusion time scales from local conditions only, because any coupling between abundances at various shells can only originate with the concentration gradient term. Likewise, for unabundant elements, it is the concentration gradient term that carries all of the memory of the distribution in evolving stars. Note that, despite its shortcomings, the approach of Paquette *et al.* (1986*a*) still leads to good estimates of diffusion time scales in cases where the abundances of heavy elements are small, the radiative forces on them are negligible, and the concentration gradients also remain small (e.g., the case of heavy metals in cool stars). In cases such as the one considered here, however, those conditions are not met, and the only relevant time scale becomes the time the system takes to reach equilibrium. We will refer to this time scale as the *relaxation time scale.* Of course, equilibrium may or may not be reached over a stellar lifetime at a given shell in a star, and the conditions for equilibrium may change as the evolution proceeds.

b) Radiative Acceleration on Helium

The calculation of the selective radiative acceleration on a given element is generally based on the assumption of local thermodynamic equilibrium. In addition, the effects of radiative transfer at small optical depths are usually neglected, and the radiative flux is then estimated from the so-called radiative diffusion approximation. As long as one limits oneself to layers below the photosphere, such simplifications are easily justified even in a very hot white dwarf. However, while these approximations greatly simplify the computations, the task of estimating g_r still remains rather involved and time consuming (see Vennes 1985). In practice, it is best to compute the radiative acceleration once and for all over a wide range of physical conditions. Even then, the simple interpolation of a relatively complicated function such as g_r in the multidimensional space of physical conditions can remain costly. This is underscored by the fact that, for computing a complete evolutionary sequence, some 4500 time steps are typically needed. Since each envelope model contains 600 shells, $\sim$2.7 million estimations of the function g_r are necessary in one sequence.

In order to keep computer costs at reasonable levels and in the spirit of exploratory work, we have adopted in our evolutionary calculations a less accurate method for estimating g_r. Instead of interpolating tabular data based on detailed calculations, the method uses an *analytic* fit which gives approximate values for g_r but is very fast to use. By sacrificing accuracy, we are still able to investigate the dominant features of evolutionary effects on the helium distribution in hot DA white dwarfs in presence of radiative levitation. In the next section, we use more detailed calculations to derive quantitatively the abundances of helium supported by radiative forces at the photospheres of such stars.

The fitting formula that we use has been developed by Michaud *et al.* (1979). Their equations (7) and (17) give the selective radiative acceleration on helium in a hydrogen plasma as a function of density, temperature, and helium-to-hydrogen number ratio. These equations are based on detailed calculations of radiative forces on helium in main-sequence stars. They give accurate results in the range of abundance $10^{-1} \geq \gamma \geq 10^{-4}$ and for temperature-density conditions typical of normal stars. In our white dwarf evolutionary models, we use the fitting formula of Michaud *et al.* (1979) outside its strict range of validity but add one modification according to a suggestion by Michaud (1982). The modification stems from the fact that the main feature of the fitting formula is a

[2] Those two terms correspond to the combined effects of the electric field and gravity and are referred to, globally, as *gravitational settling* in stellar plasmas.

dependence on abundance given by

$$g_r \propto \frac{1}{\gamma^{1/2}} . \tag{2}$$

We note that g_r can be made arbitrarily large by decreasing the abundance of helium. This means that gravitational settling can always be balanced by radiative levitation in this simple prescription. However, it is well-known that g_r reaches a limiting value when the abundance of the element being supported becomes so small that its line opacity (through which most of the support comes from) no longer affects the emergent flux. In this regime of unsaturated lines, g_r has reached a maximum value and no longer depends on the abundance of the element. In order to take this effect into account in our computations, we adopt the smallest of the radiative acceleration as given by the fit of Michaud *et al.* (1979) and a rough expression for the maximum radiative acceleration on helium derived by Michaud *et al.* (1976) and slightly modified by Michaud (1982):

$$g_r^{\max} = 1.7 \times 10^{-4}(2 - Z_2) \frac{T_e^4}{T} \frac{R^2}{r^2} , \tag{3}$$

where R is the radius of the star and the other symbols have been defined previously. A close inspection indicates that our prescription leads to quantitatively reasonable estimates of g_r in the outermost layers of very hot white dwarf models. For deeper layers and for cooler stars, such estimates are expected to deviate substantially from the predictions of more accurate calculations.

c) *Time-dependent Calculations*

Our basic model of a hot DA white dwarf envelope consists of a 0.6 $M_\odot$ stratified object made of a H-rich layer on top of a He-rich region. We investigate the temperature range $20{,}000 \leq T_e \leq 80{,}000$ K which overlaps with the observed range for hot DA/DAO stars and the region where helium levitation is expected to be significant. We follow the evolution of the helium distribution—and consequently that of the hydrogen distribution as well—by solving the mass conservation equation,

$$\frac{\partial}{\partial t}(\rho X_2) = -\frac{1}{r^2}\frac{\partial}{\partial r}(r^2 \rho X_2 w_2) , \tag{4}$$

where ρ is the density, X_2 is the mass fraction of helium, and w_2 is the diffusion velocity of helium with respect to the center of mass. The latter is given by

$$w_2 = \frac{w_{12}}{1 + (\gamma A_2)/A_1} . \tag{5}$$

The conservation equation is solved by using the finite difference scheme developed by Pelletier (1986) and briefly alluded to in Pelletier *et al.* (1986). Except for appropriate adjustments of the mesh point distribution, no difficulties were encountered in adapting this technique to a diffusion problem in presence of radiative forces. Alecian and Grappin (1984) have discussed some of the severe limitations of more standard numerical techniques for such a problem.

The initial distribution of helium in our starting model ($T_e = 80{,}000$ K) is unknown because of the well-known failure of evolution theory to provide us with realistic models of pre–white dwarf stars. For numerical convenience, we arbitrarily assume that this initial distribution is a step function. Extensive tests show that the He distribution relaxes very rapidly to a single solution in the outer layers of the model, irrespective of the initial conditions. However, in the deeper layers where radiative levitation becomes negligible, the solution does depend on the initial configuration and, in particular, on the total amount of hydrogen that is present in the envelope. In order to investigate this point, we have computed two complete evolutionary sequences corresponding to models containing quantities of hydrogen which differ by a factor 1000. The starting model for sequence A consists of a layer of hydrogen extending to a fractional mass depth $\log q (\equiv \log \Delta M/M) = -10$ and contaminated by a small, uniform amount of helium ($c_2 = 10^{-3}$). This outer layer of H-rich material surrounds a helium envelope containing a uniform trace of hydrogen ($c_2 = 0.999999$). The initial configuration for sequence B is similar except that the helium contamination in the outermost layer is smaller ($c_2 = 10^{-4}$) and that $c_2 = 0.999$ in the He-rich layer. This corresponds to a total H content some 1000 times larger than for sequence A. The base of the envelope is chosen deep enough ($\log q = -3.0$) so that the local relaxation time scale remains larger than the age of the model and the He abundance does not change there (we ignore possible interactions with a carbon core and residual nuclear burning). Consequently, our lower boundary condition is $c_2 = 0.999999$ (or 0.999) at the base of envelope. At the upper boundary, we impose no mass loss and no accretion of matter. Since we are mainly interested in the observable surface abundances of helium and since all of our models are fully radiative, this corresponds to $w_{12} = 0$ at the photosphere ($\bar{\tau} = 1$). The exact location of the layer where $w_{12} = 0$ is somewhat debatable, but is shown below to be unimportant because diffusive equilibrium is very rapidly reached in a large fraction of the outer layers. As in Pelletier *et al.* (1986), we use discrete steps in effective temperature, starting with steps of 5000 K and decreasing to steps of 1000 K following very roughly an inverse age scale. Along the evolutionary sequences, the variations in space and time of the ionic charges Z_1 and Z_2 are explicitly taken into account through the use of our tabular equations of state (see Paquette *et al.* 1986*a*). Finally, the diffusion coefficient D_{12} is evaluated from the tables of Paquette *et al.* (1986*b*).

d) *Results*

Figure 1 illustrates the early evolution of the He distribution in the starting model ($T_e = 80{,}000$ K) of sequence A. After only 1.15×10^1 yr of evolution, diffusion modifies the initial He profile (the step function labeled "0") to the distribution labeled "1." At

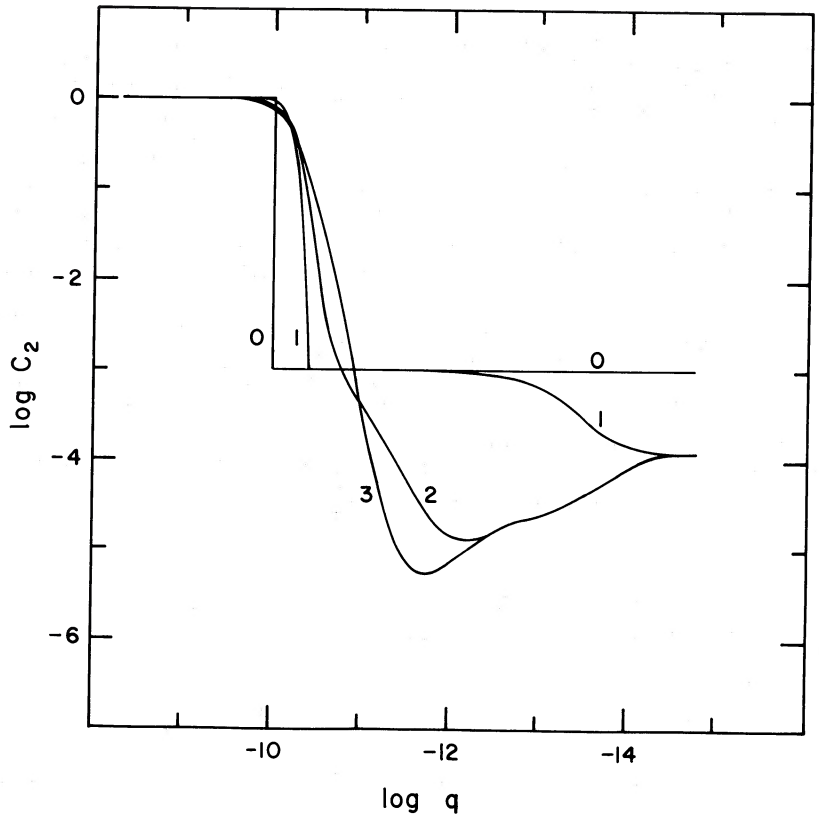

FIG. 1.—Early evolution of the helium distribution [c_2 vs. $q \equiv 1 - M(r)/M$] in the starting model of sequence A characterized by $M = 0.6\ M_\odot$ and $T_e = 80{,}000$ K. Curves labeled 0, 1, 2, and 3 correspond, respectively, to the helium distribution at time $t = 0$, 1.15×10^1 yr, 3.21×10^2 yr, and 2.37×10^6 yr (the age of the model). Only the outer part of the envelope is illustrated. The tip of the distribution on the right-hand side gives the position of the Rosseland photosphere.

the interface of the H- and He-rich layers, the concentration gradient of helium is initially so large that it pushes helium upward through ordinary diffusion. At the same time, helium sinks into the star in the outermost layers through gravitational settling, although there is already a hint in the profile that radiative levitation prevents helium from sinking further at the photosphere. This is confirmed by the curve labeled "2," which shows the helium distribution after 3.21×10^2 yr of evolution. While the helium profile still adjusts near the boundary of the H- and He-rich layers, it has frozen to a solution imposed by diffusive equilibrium in the outermost layers. The curve labeled "3" illustrates the helium distribution at the age of the 80,000 K, $0.6\ M_\odot$ model (2.37×10^6 yr). The most remarkable result of Figure 1 is that the helium distribution relaxes very rapidly to its equilibrium profile in the outermost layers. For instance, the relaxation time scale is less than 300 yr for the layers above $\log q \sim -12.5$. In the atmospheric layers themselves ($\log q \sim -14.5$), the helium abundance reaches its equilibrium value essentially instantaneously. It is to be noted that this rapid approach to diffusive equilibrium in the outer layers of our model is independent of the initial conditions as long, of course, as there is a reservoir of helium to tap. Thus, radiative levitation leads to a complete decoupling of the helium distribution: in the outermost regions, the helium abundance does not change locally and is specified by the condition $w_{12} = 0$, while separation still goes on in the deeper regions where radiative forces become negligible.

The decoupling of the surface helium distribution from the internal helium profile is dramatically illustrated in Figure 2. This figure shows the helium distribution of six models (continuous curves) belonging to sequence B ($T_e[10^3\ \mathrm{K}] = 75$, 65, 55, 45, 35, and 25, from top to bottom, respectively) and of two models (*dashed curves*) belonging to sequence A ($T_e[10^3\ \mathrm{K}] = 75$ and 25, from top to bottom, respectively). It is clearly seen that the helium distribution is specified by two different regimes. In the outermost layers, as mentioned above, the helium profile relaxes very rapidly to an equilibrium configuration provided essentially by the counterbalancing effects of radiative levitation against gravitational settling. Finite, uniquely determined amounts of helium can thus be supported at a given time in the outer layers of a DA white dwarf. As it cools, such a star loses progressively its ability to support helium in its atmosphere because its radiative flux decreases. Hence, the conditions for diffusive equilibrium change as a function of time, and, in particular, the helium distribution readjusts to these changing conditions. Figure 2 shows that radiative support is indeed less important in cooler stars, which leads to a progressive depletion of trace helium in the outer layers of a DA white dwarf. In particular, the abundance of helium at the photosphere of a DA star decreases monotonically with decreasing effective temperature.

In deeper regions, radiative levitation becomes negligible, and the approach to equilibrium is only possible through ordinary diffusion opposing gravitational settling. From equation (1), using the fact that the fractional mass depth q scales linearly with the pressure, considering only small abundances ($c_2 \ll 1$, $c_2 \approx \gamma$), assuming an ideal, nondegenerate gas, and taking $g_r = 0$, it can be

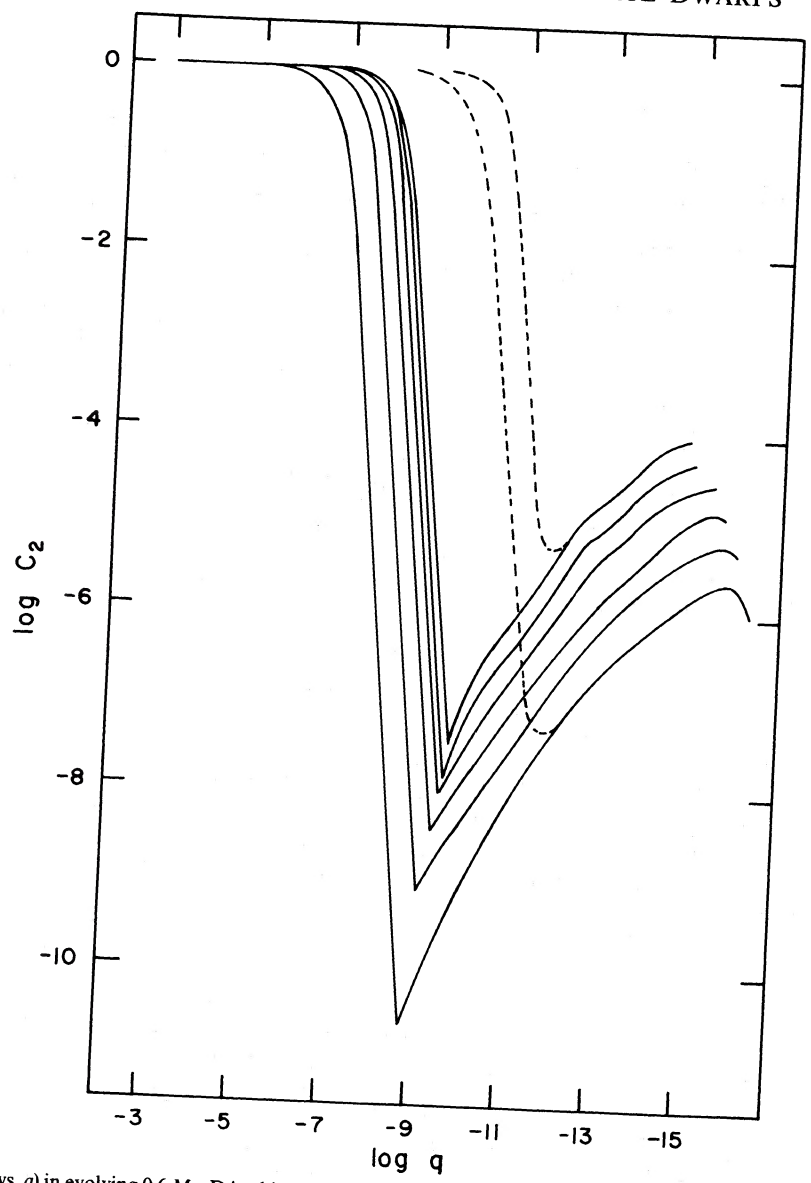

FIG. 2.—Helium distributions (c_2 vs. q) in evolving 0.6 $M_\odot$ DA white dwarfs. Continuous curves correspond to sequence B models ($T_e[10^3$ K] = 75, 65, 55, 45, 35, and 25, from top to bottom, respectively), and dashed curves to sequence A models ($T_e[10^3$ K] = 75 and 25, from top to bottom, respectively).

shown (see below) that the equilibrium condition $w_{12} = 0$ leads to the relationship

$$c_2 \propto q^\beta , \tag{6}$$

where

$$\beta = \frac{A_2}{A_1}(Z_1 + 1) - Z_2 - 1 . \tag{7}$$

For trace He III in a background of H II, $\beta = 5$. That the system tends to evolve toward an equilibrium state is indicated in Figure 2 where the tail of the helium distribution assumes indeed a slope of 5 (excluding the outer layers where radiative levitation is important). The small differences that are observed between the slopes of various distributions correspond simply to small differences in the average charge of helium (Z_2) from shell to shell and from one model to another; Z_2 is not exactly equal to 2 and decreases somewhat with cooling (thus increasing the slope as observed). Hence, the helium distribution in the deeper layers is specified by the opposing tendencies induced by gravitational settling and ordinary diffusion. However, in the two sequences considered, equilibrium is clearly not reached over the time span covered by our calculations since H and He are still separating (the helium distribution at large depths would practically not change with decreasing effective temperature if equilibrium had been reached there). Because there is 1000 times more hydrogen migrating upward from the deep envelope in the models belonging to sequence B (*continuous curves*) than in the models belonging to sequence A (*dashed curves*), the separation is much less complete in

the former sequence, as can be clearly seen in Figure 2. Whereas the helium distribution at large depths depends on the initial configuration, note again that the distribution supported by radiative levitation does not. This is illustrated by the convergence of the solutions for the 75,000 K and 25,000 K models belonging to both sequences in Figure 2. In addition, note that the transition from the regime in which gravitational settling is opposed by ordinary diffusion to the regime in which it is opposed by radiative levitation is very sharp in the sequence B models. This transition remains also sharp for the sequence A models although at a somewhat reduced level as indicated by the relatively flat minima of the dashed curves.

It seems worth mentioning that the He/H ratio at the photosphere of a hot DA white dwarf with a relatively thick layer of hydrogen such as the models considered here would decrease at catastrophic rates with decreasing effective temperature if radiative levitation was ignored. This was done, for example, by Iben and MacDonald (1985), who find a very steep functional dependence $\mathrm{He/H} \sim T_e^{40}$ in hot DA white dwarfs. Such a dependence is not appropriate for the atmospheric layers where radiative support cannot be neglected. However, the result of Iben and MacDonald (1985) is not necessarily at variance with the present results if deeper layers are considered. For example, Figure 2 indicates that at the Lagrangian mass point $\log q = -11.0$, the local helium abundance in sequence A models scales as $\mathrm{He/H} \sim T_e^6$ in the effective temperature interval 25,000 K $\leq T_e \leq$ 75,000 K. The dependence is $\mathrm{He/H} \sim T_e^{16}$ for sequence B models at $\log q = -8.5$ in the same temperature interval. It thus appears that the result of Iben and MacDonald could be appropriate for a given mass shell and for a given configuration since the results are sensitive to the initial conditions.

The most important result of this section, however, is the demonstration that the relaxation time scale is extremely short in the outermost layers of stars where radiative levitation is important. This means that in the absence of other competing mechanisms such as accretion or mass loss, the distribution of a given levitating element freezes to its equilibrium configuration in these layers. As a consequence, the surface abundances become totally decoupled from the evolving internal distribution. One can thus safely utilize *static* models to study the various patterns of trace elements that may levitate in the atmospheres of hot white dwarfs. This basic conclusion is totally independent of the approximate treatment of g_r that we have used here.

III. RADIATIVE LEVITATION OF HELIUM IN HOT DA WHITE DWARFS

a) Theoretical Predictions

The results of the previous section allow us to study in a more quantitative way the question of the expected helium abundance supported by radiative levitation in the atmospheric layers of a hot DA white dwarf. Because it has been established that the use of (inexpensive) static models suffices for the task, we now do away with the simplified prescription of g_r introduced in the evolutionary calculations and compute equilibrium helium abundances from detailed calculations of g_r obtained specifically for the present paper. Our calculations of the selective radiative acceleration exerted on helium in a stellar hydrogen plasma use, with some changes, the same input physics as that employed by Michaud *et al.* (1979). In particular, in both cases, the results are valid for optically thick plasmas (the radiative diffusion approximation) and for conditions of local thermodynamic equilibrium. However, the region of density-temperature covered by our white dwarf models is much larger than that considered by Michaud *et al.* (1979) for their main-sequence star models. In addition, we have introduced a model of pressure ionization to deal with some of the more extreme physical conditions that are encountered in white dwarfs. Details of this and of the computations of monochromatic opacities, line broadening, and redistribution processes can be found in Vennes (1985).

The results of our detailed computations of the radiative acceleration on helium are available in the form of a three-dimensional table which gives g_r as a function of density, temperature, and helium-to-hydrogen number ratio over a wide range of parameters. The table covers a diagonal region in the density-temperature plane defined by $4.2 \leq \log T \leq 7.0$, and the following formula: $\log \rho = 4.3 \log T - 27.5 \pm 2.5$. This covers completely the region of interest for our white dwarf models. The He/H ratio is restricted to $\gamma \leq 10^{-1}$. The smallest value of γ that we have considered in practice is 10^{-9}, corresponding to complete desaturation of the helium lines. One important advantage of the present calculations over the approximate treatment presented in § II*b* is that our estimates of g_r are substantially improved from a quantitative point of view. This is particularly significant in view of the fact that our white dwarf models cover mostly regions of parameter space which are outside the strict range of validity of the fitting formula of Michaud *et al.* (1979). One further advantage is that the present calculations offer a natural description of desaturation effects via the exact numerical relationship between g_r and γ. This is to be contrasted with the cruder prescription of the previous section which imposes the relationship $g_r \propto \gamma^{-1/2}$ until the radiative acceleration has grown larger than the value given by equation (3).

We use our improved estimates of g_r in conjunction with the condition of diffusive equilibrium which is expected in the outer layers of our models as demonstrated in the previous section. Noting that only small amounts of helium are supported in these layers ($c_2 \ll 1, \gamma \ll 1$), we have,

$$\frac{\partial \ln p_i}{\partial r} = \frac{\partial \ln p_1}{\partial r} = -\frac{A_1}{(Z_1 + 1)} \frac{m_p g}{kT}, \tag{8}$$

and the equilibrium condition ($w_{12} = 0$) can be written, from equation (1),

$$\frac{-\partial \ln c_2}{\partial r} - \left[A_2 - A_1 \frac{(Z_2 + 1)}{(Z_1 + 1)} \right] \frac{m_p g}{kT} + \frac{A_2 m_p g_r}{kT} = 0 . \tag{9}$$

Although the concentration gradient term is not strictly equal to zero in the outermost layers of our models, it is actually quite small as compared to the other terms, and the equilibrium condition reduces to

$$g_r = \left[1 - \frac{A_1}{A_2} \frac{(Z_2 + 1)}{(Z_1 + 1)} \right] g . \tag{10}$$

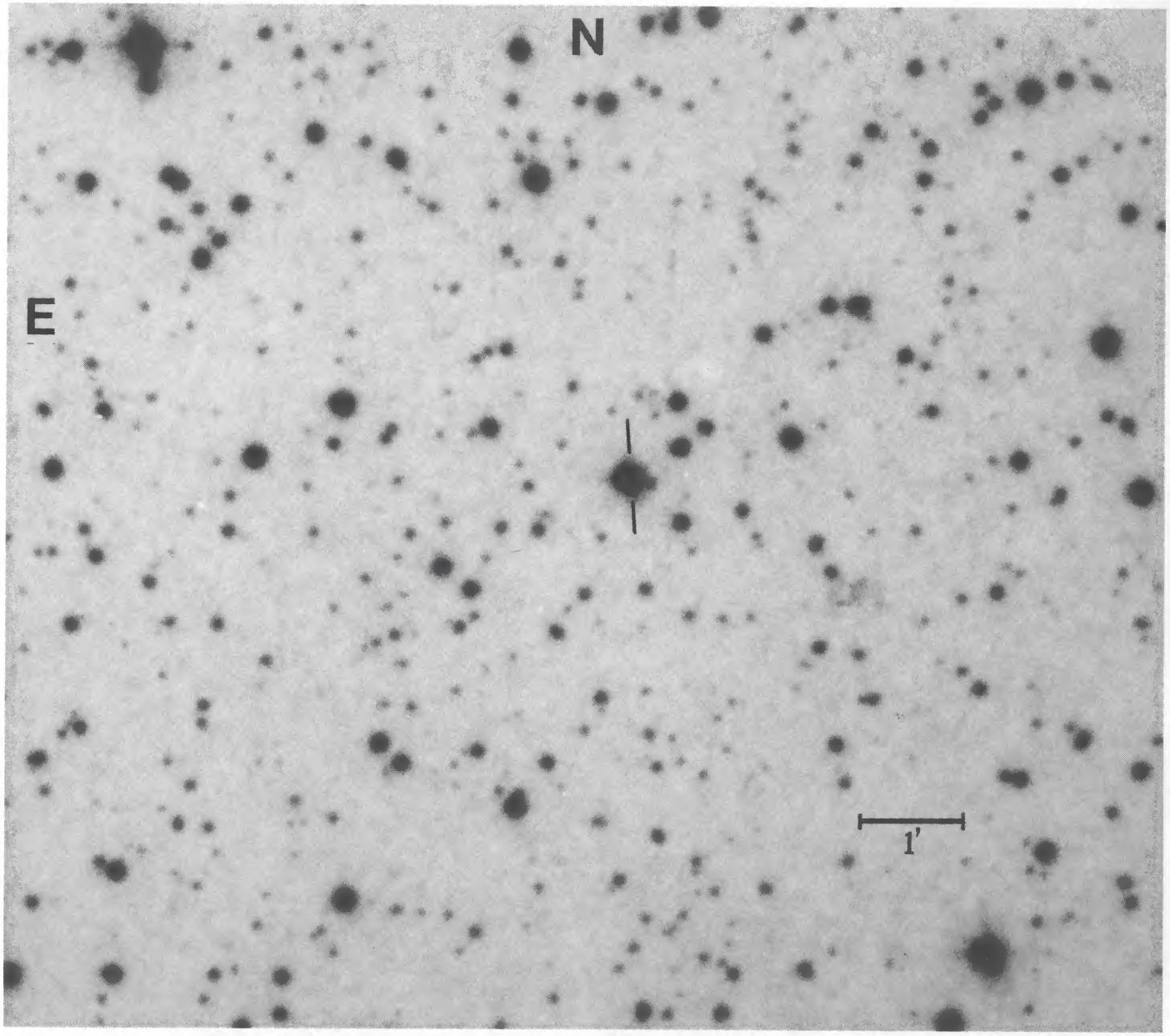

FIG. 1.—Finding chart for 18095+2704, reproduced from the Palomar Observatory Sky Survey red (E) print. The scale is indicated on the lower right. The 1950.0 coordinates are R.A. = $18^h09^m31^s.0$ and decl. = $+27°04'30''$.

pfahl and D. Welch with the DAO radial velocity spectrometer. These yield a mean heliocentric radial velocity of -30 ± 2 km s^{-1}, with an indication of variability.

Ground-based photometric observations have also been obtained. Intermediate-band *uvby* observations were undertaken by E. Olson and P. Etzel on three nights in 1987 June and July with the 1.0 m telescope at Mount Laguna Observatory. The *v* filter was nonstandard, centered 100 Å longward of the standard one. Differential photometry with respect to HD 161817 (Philip and Philip 1973) led to the mean magnitudes listed in Table 1 along with the standard deviations of a single observation. The object is variable in light with an observed range of 0.07 mag in *y*. The individual photometric observations, along with the individual radial velocity values, will be included as part of a longer term study of the variability of this object. Subsequently, one of us (B. J. H.) observed the object with the 0.6 m telescope at Yerkes Observatory, obtaining *B* and *V* magnitudes on the standard Johnson system. These are also listed in Table 1. A conversion to flux was accomplished for the *B* and *V* measurements using the calibration of Hayes (1979). The *uvby* flux conversion was performed by deriving the flux relative to that through the *y* band, following the procedures of Olson (1982) and based upon Kurucz (1979) model atmospheres for 6000 to 7000 K supergiants. The *y* band calibration was assumed to be the same as that of *V*, which is sufficiently close for our purposes. The object has an observed $(B-V)$ value of $+1.03$. Assuming that $(B-V)_0 = 0.25$, an average value derived from the tabulation of FitzGerald (1970) and Johnson (1966), yields $E(B-V)$ of 0.78. In comparison, the contribution from interstellar reddening in this region is esti-

unavoidable. However, for our present needs, we estimate that the average value of the He/H ratio in the atmospheric layers of a hot DA white dwarf can be obtained, within a factor 2–3, from its equilibrium value at the Rosseland photosphere ($\bar{\tau} = 1$). In general, the helium abundance at the deeper EUV/soft X-ray photosphere is less than that at the Rosseland photosphere if the helium distribution is specified by radiative forces as is the case here.

Figure 4 shows the predicted helium-to-hydrogen number ratio at the photosphere of DA white dwarf models as a function of effective temperature. The curve that is qualitatively different from the others in the sense that it extends to $T_e \sim 20{,}000$ K, summarizes the results of the evolutionary calculations of the 0.6 $M_\odot$ models discussed in the previous section (see also Fig. 2). The other curves refer to equilibrium abundances derived from equation (10) and our detailed calculations of g_r. The middle continuous curve shows the results for a sequence of models with $M = 0.6\ M_\odot$. Note that the gravity is not constant along this sequence but varies according to the calculations of Winget, Lamb, and Van Horn (1988). A comparison of this curve with the results of the previous section shows that our approximate description of g_r indeed gives reasonable results for very hot models, but that the radiative support on helium becomes increasingly overestimated with decreasing effective temperature. This can again be traced back to the crude treatment of desaturation effects in the calculations of the radiative acceleration.

The upper and lower continuous curves give, respectively, the expected helium abundance in the same 0.6 $M_\odot$ models, after arbitrarily multiplying and dividing our values of g_r by a factor 3. We believe that this corresponds to a realistic (and perhaps even generous) estimate of the intrinsic error in the computations of the radiative acceleration on helium in our white dwarf models. The two other sets of curves are similar, except that they refer to sequences of models with 0.4 $M_\odot$ (*dashed lines*) and 0.8 $M_\odot$ (*dotted lines*), respectively. This range of mass covers the domain in which most of the white dwarfs are found, as is well known. As expected, helium levitation is less efficient in more massive stars because of their higher gravities. It may be noted, however, that the spread in predicted abundances is not as large as might be naively suspected because the additional line broadening and corresponding increased support found in the higher gravity atmospheres provides a partially compensating effect.

Figure 4 shows that small traces of helium can be supported by radiative levitation in the atmospheres of hot DA white dwarfs. In general, the higher the effective temperature, the higher the helium abundance. By the time such a star has cooled down to $T_e \sim 40{,}000$ K, it has essentially lost its ability to support substantial amounts of helium in its atmosphere. Note that this ability is also lost at very high effective temperatures because only a very small amount of helium can remain in the He II state through which

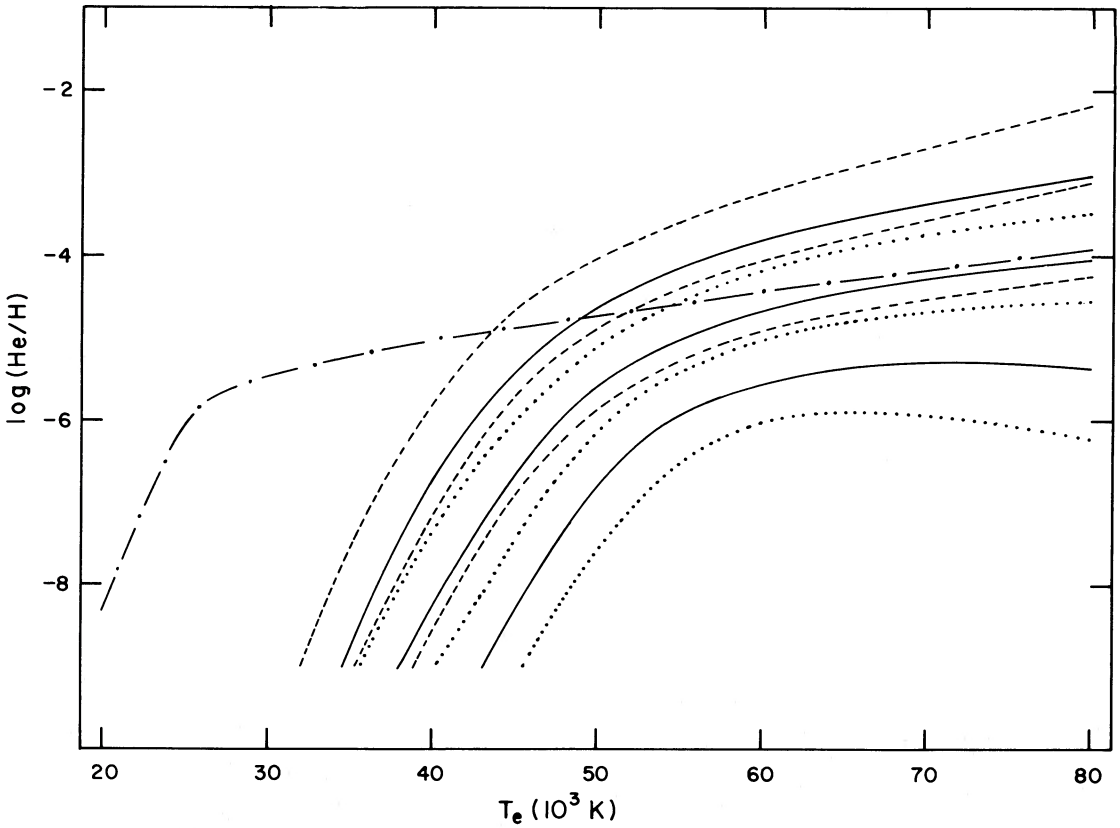

FIG. 4.—Predictions of radiative force calculations. Diagram shows the expected He/H ratio at the photosphere of DA white dwarfs as a function of effective temperature. Middle continuous curve shows the results obtained from detailed calculations of the radiative acceleration for a sequence of models with $M = 0.6\ M_\odot$. Long dashed-dotted line corresponds to similar results but derived from our approximate prescription for the calculation of the radiative acceleration on helium. Upper and lower continuous curves give, respectively, the expected helium abundance in the same 0.6 $M_\odot$ model after multiplying and dividing our values of the radiative acceleration by a factor of 3. This gives a measurement of our estimated errors in our computations. The two other sets of curves are similar, except that they refer to sequences of models with $M = 0.4\ M_\odot$ (*dashed lines*) and $M = 0.8\ M_\odot$ (*dotted lines*), respectively.

TABLE 1

COMPILATION OF INFERRED HELIUM ABUNDANCES IN HOT DA WHITE DWARFS

WD Number	Name	$T_e(10^3$ K)	log g	He/H (10^{-5})	Data	References
0004+330.....	GD 2	40:	(8.0)	<2	EX	1
0050−332.....	GD 659	35–39	(8.0)	0.5–4.2	EX	2
		35–38	(8.0)	<2	EX	3
0232+035.....	Feige 24	50–60	(8.0)	3–300	E (EX)	4 (see also 5)
0302+027.....	Feige 31	26–35	(8.0)	<15	EX	3
... .	LB 1663	35–39	(8.0)	4.3–14.7	EX	2
		35–39	(8.0)	10–20	EX	3, 6
		35–39	(8.0)	2–60	E	7
0346−011.....	GD 50	45–50	(8.0)	30–200	E	7
0501+527.....	G191-B2B	52–68	(8.0)	350–930	EX	2
		55–66	(8.0)	>320	EX	3
0548+000.....	GD 257	50–60	(8.0)	50–250	EX	3
		50–60	(8.0)	80–600	E	7
0549+158.....	GD 71	32–35	(8.0)	<3.2	EX	3
0612+177.....	G104-27	24–27	(8.0)	>6	EX	3
0642−166.....	Sirius B	25–26	8.5–8.7	<2	EX	3, 8
		27.5	(8.0)	<1	EX	9
1031−115.....	LTT 3870	25.5:	(8.0)	<1	EX	1
1052+273.....	GD 125	24–28:	(8.0)	1–5	E	4
1254+233.....	GD 153	40–44	(8.0)	2.2–8.4	EX	2
		38.5–41.0	(8.0)	0.6–2.0	EX	3
		40–44	(8.0)	2–40	E	7
1314+293.....	HZ 43	54–60	(8.0)	4–66	EX	2
		45–54	8.0–9.0	<1	EX	3, 10
		59–62	(8.0)	<0.6	EX	11
1544+008.....	LB 898	36–42:	(8.0)	>2	E	4, 7
1620−391.....	CoD −38°10980	24.5	(8.0)	<0.5	EX	6
1658+441.....	PG 1658+441	28.5–32.5	(8.0)	<2	EX	3
		26–30	(8.0)	<10	EX	12
1936+327.....	GD 222	45–50:	(8.0)	>100	E	4
2028+390.....	GD 391	24–30	(8.0)	0–7	EX	2
		24–30	(8.0)	<10	EX	3
2111+498.....	GD 394	35–37	(8.0)	3.2–7.2	EX	2
		35–37	(8.0)	2.1–4.8	EX	3
2240−045.....	Feige 106	32–42	(8.0)	>10	EX	3
		32–42	(8.0)	>30	E	4
2309+105.....	GD 246	50–60	(8.0)	30–144	EX	2
		52–59	(8.0)	60–130	EX	3
		50–60	(8.0)	15–150	E	4
... .	V471 Tauri	33–37	(8.0)	<3	EX	13

REFERENCES.—(1) Petre and Shipman 1987. (2) Jordan *et al.* 1987. (3) Paerels and Heise 1988. (4) Petre, Shipman, and Canizares 1986. (5) Paerels *et al.* 1986*b*. (6) Paerels *et al.* 1987. (7) Kahn *et al.* 1984. (8) Paerels *et al.* 1988. (9) Heise 1985. (10) Heise *et al.* 1988. (11) Paerels *et al.* 1986*a*. (12) Pravdo *et al.* 1986. (13) Jensen *et al.* 1986.

most of the radiative support originates. Such an ionization effect is responsible for the turnover of the two lower curves at high effective temperatures in Figure 4.

b) Comparison with the Observations

We have compiled the result of all published analyses of hot DA white dwarfs observed with the *Einstein* and/or *EXOSAT* satellite. With the exception of two stars, we obtain a sample of 24 objects found in the range 24,500 K $\lesssim T_e \lesssim$ 62,000 K. In all cases, helium is spectroscopically invisible in these stars, and its abundance has been inferred from the opacity it would provide to account for the observed short-wavelength flux. Table 1 summarizes our compilation. The first column gives the WD number according to the designation of McCook and Sion (1984) if the star is listed in their catalog. The second column gives the usual name of the object. The third and fourth columns list, respectively, the effective temperature and surface gravity used in the various abundance analyses. It is to be noted that, with the exception of Sirius B and HZ 43, the canonical value log $g = 8.0$ has been used in all other studies. The fifth column gives the inferred atmospheric He/H ratio (or appropriate limits). Finally, the sixth column indicates the data source ("EX" for *EXOSAT* and "E" for *Einstein*), and the last one gives reference to the relevant papers.

The two stars left out of Table 1 deserve some comments. Although the object GD 691 (WD 0109−264) was reported by Petre and Shipman (1987) as a null *EXOSAT* detection and a lower limit on the He/H ratio was correspondingly inferred, Lyα observations by Holberg and Wesemael suggest that this object may in fact be a subdwarf and not a DA white dwarf. As for the faint DA star WD 1910+047 discussed by Margon, Bolte, and Anderson (1987), there appears to be enough uncertainty concerning the true nature of this object that we have preferred not to include it in Table 1 at this stage.

Table 1 indicates that half of the stars in the sample have been analyzed more than once. Except for HZ 43, the results of these independent analyses are remarkably consistent, even in those cases where the data sources are different (*EXOSAT* vs. *Einstein*). Because of this, we feel confident that we can rely on individual He/H determinations irrespective of their sources, and that we can

average the inferred helium abundances in the case of multiply analyzed stars. In this averaging process, we have not discriminated against the less sensitive *Einstein* results. Also we have chosen to use actual determinations as opposed to limits in individual cases where both were derived from independent (but consistent) analyses.

The results of this procedure are shown in Table 2 where we list the adopted helium abundance for each of the 24 stars in the sample. Effective temperatures and gravities are reported from Table 1 except for 10 stars whose parameters have been taken from the work of Holberg, Wesemael, and Hubený (1984) and of Holberg, Wesemael, and Basile (1986). Note that these parameters are not necessarily those used in the individual analyses of short-wavelength observations. However, they are based on Lyα line profile observations and, as such, are currently the best values for hot DA white dwarfs.

We have added, in Table 2, the results of the analysis of Wesemael, Green, and Liebert (1985) concerning the three known DAO stars. Contrary to the other stars listed in the table, these three objects show helium features in their spectra. With the addition of these objects, Table 2 represents the largest sample of stars from which one can study the helium abundance pattern in hot DA/DAO white dwarfs.

Figure 5 shows a plot of the inferred atmospheric He/H ratio as a function of effective temperature for the 24 DA stars listed in Table 2. Actual determinations are represented by filled circles, while lower and upper limits on He/H are represented by upward- and downward-pointing arrows, respectively. The dashed arrow associated with HZ 43 reflects the difficulty encountered by Jordan *et al.* (1987) to reconcile their analysis with that of Paerels *et al.* (1986*a*) which favors an upper limit He/H $\lesssim 6 \times 10^{-6}$. (In this context, however, the nonvisibility of the 227 Å He II edge in the *EXOSAT* spectrum of HZ 43 leaves little doubt that the atmospheric helium abundance is less than He/H $\sim 10^{-5}$; Heise *et al.* 1988.) The open circles give the results for the three DAO stars listed in Table 2. In order to avoid confusion, we have not plotted individual error boxes. Instead, the box shown in the upper left corner of the figure typifies the average error of our 27 objects.

Except perhaps for HZ 43, Figure 5 suggests a definite correlation in the sense that more abundant traces of helium are found in the atmospheres of hotter DA white dwarfs. Petre, Shipman, and Canizares (1986) and, more recently, Petre and Shipman (1987) have discussed this same correlation using smaller samples of stars. By contrast, Jordan *et al.* (1987) and Paerels and Heise (1988), also using smaller samples (which may have the advantage of being more homogeneous), choose to speak of a simple trend characterized by a low-temperature group ($T_e \lesssim 45{,}000$ K) in which the stars have approximately the same helium abundance (He/H $\sim 10^{-5}$–10^{-4}) and a high-temperature group in which the helium abundance is some 100 times larger, but, again, with no obvious correlation with effective temperature. Amusingly, however, a correlation between He/H and T_e is apparent to us when we look at Figure 4 of Paerels and Heise (1988). In any case, we prefer to interpret the results of Figure 5 as a true positive correlation between helium abundance and effective temperature, a correlation that has become even more suggestive than before by adding here the three DAO stars. We note after several authors that the scatter is substantial, however.

For comparison, we have also plotted in Figure 5 the expected helium abundance supported by radiative forces at the photospheres of DA white dwarf models with $M = 0.4$, 0.6, and 0.8 $M_\odot$, respectively (*solid lines*). The three curves shown are simply a subset of the curves produced in Figure 4. They demonstrate that radiative levitation of helium fails to explain the observations by some two orders of magnitude even under the most favorable circumstances (i.e., at high effective temperatures). The discrepancy

TABLE 2

ADOPTED PARAMETERS FOR HOT DA/DAO WHITE DWARFS

Name	T_e (10^3 K)	log g	log (He/H)
GD 2	40:	(8.0)	< -4.70
GD 659	37 ± 2	8.17 ± 0.30	-4.84 ± 0.46
Feige 24	55 ± 5	7.23 ± 0.35	-3.52 ± 1.00
Feige 31	30.5 ± 4.5	(8.0)	< -3.82
LB 1663	37 ± 2	(8.0)	-3.88 ± 0.38
GD 50	47.5 ± 2.5	(8.0)	-3.11 ± 0.41
G191−B2B	62 ± 4	7.55 ± 0.35	-2.24 ± 0.22
GD 257	55 ± 5	(8.0)	-2.78 ± 0.41
GD 71	33.5 ± 1.5	(8.0)	< -4.49
G104−27	25.5 ± 1.5	(8.0)	> -4.22
Sirius B	27 ± 1	8.65 ± 0.15	< -4.82
LTT 3870	25.5:	(8.0)	< -5.00
GD 125	26 ± 2:	(8.0)	-4.65 ± 0.35
GD 153	42 ± 2	8.23 ± 0.30	-4.28 ± 0.51
HZ 43	57 ± 3	8.5:	$< -5.10, 3.79$
LB 898	39 ± 2:	(8.0)	> -4.70
CoD −38°10980	24.5	8.08 ± 0.15	< -5.30
PG 1658+441	29 ± 3	(8.0)	< -4.22
GD 222	47.5 ± 2.5:	(8.0)	> -3.00
GD 391	27 ± 3	(8.0)	< -4.15
GD 394	36 ± 1	8.13 ± 0.23	-4.40 ± 0.18
Feige 106	37 ± 5	(8.0)	> -3.70
GD 246	54 ± 3	7.64 ± 0.45	-3.15 ± 0.30
V471 Tauri	35 ± 2	8.25 ± 0.25	< -4.52
Abell 7	60 ± 10	~7	-2.20 ± 0.15
PG 1210+533	50 ± 10	~8	−1.70
HZ 34	60 ± 10	~7	-1.70 ± 0.20

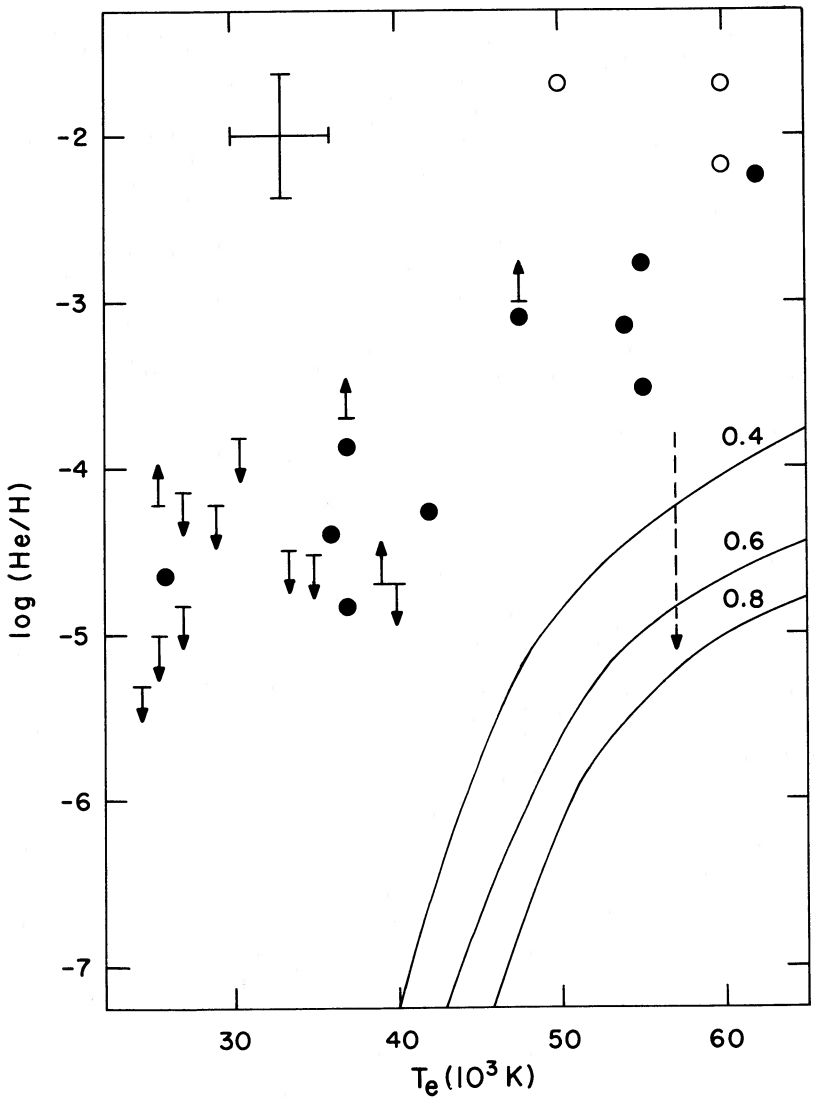

FIG. 5.—Helium abundance in the atmospheres of hot DA white dwarfs (He/H vs. T_e). Filled circles and arrows give the helium abundance (or corresponding limits) inferred in 24 hot DA white dwarfs observed at soft X-ray wavelengths. Open circles correspond to the helium abundances measured in three DAO objects. Error box is the average of the individual boxes. The three continuous curves correspond to the predicted helium abundances supported by radiative forces in sequences of models with $M = 0.4$, 0.6, and 0.8 $M_\odot$, respectively. Quite clearly, helium radiative levitation fails to explain the observations.

grows larger for $T_e \lesssim 40{,}000$ K, where radiative levitation of helium becomes practically negligible in DA white dwarfs. Pushing the uncertainties of our computations of g_r in the right direction increases somewhat the expected abundances (see Fig. 4), but still cannot account for the observations. Likewise, we believe that more detailed calculations of radiative forces (including perhaps non–LTE and radiative transfer effects) will not change the present qualitative picture. Thus, we reach the central conclusion of this section: the abundances of helium inferred or measured in the atmospheres of hot DA/DAO white dwarfs cannot be explained by helium radiative levitation. In the next section, we examine alternate possibilities.

It is important to point out that, irrespective of its failure to account for the observations, radiative levitation does provide a *minimal* amount of helium in the atmospheres of hot DA white dwarfs. As long as mass loss and accretion can be neglected and access to a helium reservoir is secured, diffusion always brings to the surface quantities of helium consistent with diffusive equilibrium. In a DA white dwarf, the He-rich region below the H-rich outer layer is, of course, the natural reservoir of helium. In the absence of competing mechanisms, the minimal helium pollution provided by radiative support cannot be ignored. In this context, it is worth mentioning that the upper limit He/H $\lesssim 6 \times 10^{-6}$ derived by Paerels *et al.* (1986*a*) for HZ 43 remains consistent with our calculations. And indeed, Figure 5 shows that the tip of the arrow for HZ 43 almost touches the theoretical curve for the 0.8 $M_\odot$ models. At $T_e = 57{,}000$ K, a model with $M = 0.8\ M_\odot$ has $\log g \sim 8.3$. Because HZ 43 has still a higher gravity (see Table 2), the theoretical helium abundance supported by radiative levitation must indeed be smaller than He/H $\sim 6 \times 10^{-6}$.

IV. THE CASE FOR THIN HYDROGEN LAYERS IN DA WHITE DWARFS

a) Alternatives to Radiative Support

We have demonstrated that the abundances of helium that can be supported by radiative forces in the atmospheres of hot DA white dwarfs are too small to account for the observations. We must then find another mechanism able to compete more efficiently against gravitational settling. In the case of the 24 objects for which the presence of helium has been inferred on the basis of a required EUV/soft X-ray opacity source, radiative levitation should not be written off too soon. And, indeed, we expect that other elements such as C, N, and O can also levitate in hot DA atmospheres (e.g., Vauclair, Vauclair, and Greenstein 1979), so that the resulting soft X-ray opacity could very well be substantially larger than that provided by helium levitation alone. We note that at least three of the stars considered (Feige 24, G191-B2B, and GD 394) do show metallic features in their spectra. It remains to be seen whether the cumulative effects of levitating elements such as He, C, N, O, and Si are sufficient to quench and regulate the soft X-ray flux of hot DA stars and explain the observed correlation between the effective temperature and the abundance of the "absorber" (assumed to be helium in the available analyses). The detailed investigation of radiative forces on various heavy elements in white dwarf atmospheres being carried out by Chayer (1987) should go a long way toward answering this question. There are already hints, however, that radiative levitation is not the full story. And indeed, the results of Chayer *et al.* (1987) indicate that selective radiative forces can account for the observed surface abundances of N and Si in Feige 24,[3] but that the predicted abundance of C is some 50 times larger than the observed one. The implication is that radiative levitation and gravitational settling are not the only important mechanisms at work in the outer layers of this particular star. Paerels *et al.* (1986*b*) also have difficulties in interpreting the EUV spectrum of Feige 24 in terms of a H-rich model atmosphere with traces of C, N, and Si at the levels determined by Wesemael, Henry, and Shipman (1984). Although they make the point that the distributions of C, N, and Si have been assumed to be uniform in their model while such distributions may actually show some dependence on depth, this restriction does not appear really critical in the context of the radiative levitation model since Chayer (1987) has shown that the equilibrium distributions of heavy elements in the atmosphere of Feige 24 are relatively flat. Again, this suggests that something else is at work in Feige 24 besides settling and radiative levitation. Nevertheless, more detailed models are needed to fully understand the effects of heavy elements as short-wavelength opacity sources in hot white dwarfs. We note that the possibility that absorbers other than helium can play a significant role in determining the EUV/soft X-ray energy distribution of a hot DA white dwarf has also been alluded to by Kahn *et al.* (1984), Petre, Shipman, and Canizares (1986), and Jordan *et al.* (1987). Irrespective of this possibility, however, the need for a mechanism to support helium other than radiative levitation is unavoidable for the DAO stars, the natural progenitors of hot DA white dwarfs.

Accretion of interstellar matter is one process which can, under appropriate circumstances, counterbalance the effects of gravitational settling in white dwarfs. And, indeed, it appears to be the only plausible process that can account for the presence of traces of metals in the spectra of several cool white dwarfs (see Paquette *et al.* 1986*a*, and references therein). However, there are a number of compelling reasons against the occurrence of accretion onto hot white dwarfs, the most important of which is the evidence brought forward by Bruhweiler and Kondo (1983) in favor of *winds* or *static halos* in hot ($T_e \gtrsim 20{,}000$ K) DA white dwarfs. Kahn *et al.* (1984), Paerels *et al.* (1986*a*, *b*), Paerels and Heise (1988), and Petre, Shipman, and Canizares (1986) have all considered accretion as a possibility for maintaining finite amounts of helium in the atmospheres of hot DA stars. In particular, the latter authors do not favor (but cannot totally rule out) accretion as a viable mechanism. We can do just that, i.e., rule out accretion, in the case of DAO stars. The usual argument is to assume that a mass fraction X^p of accreted element (helium in the present case) is maintained at the photosphere of a star through a steady state situation between accretion and gravitational settling. The photospheric abundance of the element is related to its mass fraction X^a in the accreting material by the relation (see Paquette *et al.* 1986*a*, eq. [29]),

$$\frac{X^p}{X^a} = \frac{\theta}{Mq}\left(\frac{dM}{dt}\right), \tag{11}$$

where θ is the settling time scale at the photosphere, M is the total mass of the star, q is the fractional mass contained in the atmosphere, and dM/dt is the accretion rate. Following the same procedure as in Paquette *et al.* (1986*a*) and assuming that helium is accreted in solar proportions ($X^a = 0.28$), we find that an accretion rate $dM/dt \sim 1.6 \times 10^{-16}\ M_\odot\ \mathrm{yr}^{-1}$ is necessary to maintain a photospheric abundance He/H $= 10^{-2}$ ($X^p = 3.9 \times 10^{-2}$) in a DA model with $M = 0.6\ M_\odot$ and $T_e = 60{,}000$ K, parameters typical of DAO objects. Such an accretion rate is unreasonably large for a typical white dwarf, considering that, during most of its lifetime, the latter will be traveling through the hot, tenuous interstellar medium from which only accretion rates 3 to 4 orders of magnitude smaller than this figure can be expected (Wesemael 1979). The situation is even more severe for a *hot* white dwarf because its lifetime is *less* than the typical time between cloud encounters ($\sim 5 \times 10^7$ yr) during which higher accretion rates may be expected. If one nevertheless insists that an accretion rate of $1.6 \times 10^{-16}\ M_\odot\ \mathrm{yr}^{-1}$ is possible onto a DAO star, then not only does one get a photospheric helium abundance He/H $= 10^{-2}$, but also carbon, nitrogen, and oxygen abundances reduced by about only a factor 10 as compared to their solar values. This assumes accretion of matter in solar proportions and uses the same arguments as were used for helium (eq. [11]), this time for the C IV, N V, and O V ions which are typical of the conditions encountered in DAO atmospheres. These large traces of carbon, nitrogen, and oxygen are not detected in DAO stars[4] and argue, at the very least, against

[3] Feige 24 is the only object of the present sample for which detailed abundance analyses of heavy elements have been carried out (see Wesemael, Henry, and Shipman 1984).

[4] PG 1210+533 is the only DAO star observed up to now with the *IUE* in the high-resolution mode. Holberg, Sion, and Vauclair (1987) and Holberg (1987*b*) report that no convincing features of common heavy elements (C, N, O, Si) are present in a 13 hr SWP exposure of this star at the 100 mÅ level. If C and N in particular were present at 10% of their solar abundances in the atmosphere of PG 1210+533, several prominent features would have been easily detected according to the calculation of Henry, Shipman, and Wesemael (1985). For example, from their tables, assuming $T_e = 60{,}000$ K, we find the following equivalent widths: 656 mÅ (C III, λ1577), 1020 mÅ (C IV, λ1549), 175 mÅ (N V, λ1240).

accretion in solar proportions. From these arguments, we conclude that accretion is an unlikely mechanism for explaining the presence of helium in the atmospheres of DAO stars and, presumably, in the atmospheres of their cooler counterparts, the hot DA stars. We note that an accretion rate $dM/dt \sim 2.2 \times 10^{-19}\ M_\odot\ \mathrm{yr}^{-1}$ would suffice to maintain an abundance He/H = 10^{-5} at the photosphere of a 30,000 K, 0.6 $M_\odot$ DA white dwarf model. While this rate may appear more comfortable than the value required for DAO objects, it seems unappealing to invoke two different mechanisms to account for the same phenomenon. Also, and independently of the results of Bruhweiler and Kondo (1983), it is doubtful that an isolated star with $T_e \gtrsim 30{,}000$ K can accrete at all because of its radiative flux and associated H II region.

The effects of mass loss on the spectral evolution of white dwarfs and, in particular, the interaction between mass loss and gravitational settling remain to be investigated. Some qualitative understanding of this process is already possible, however. If we refer to Figure 2, we can think of the helium distribution in terms of two (weakly) connected reservoirs of helium. If the mass-loss rate is relatively small, then we can imagine that the wind can only tap the outer reservoir (that supported by radiative levitation) over the time span corresponding to the cooling age of, say, a 25,000 K star. In that case, the photospheric abundance of helium along the cooling sequence can only remain comparable to (or become smaller than) the abundance supported by radiative forces by virtue of the decreasing value of c_2 with increasing depth. On the other hand, if the mass-loss rate is sufficiently large, then the wind empties very quickly the outer reservoir and starts tapping the inner one. When this happens, the photospheric helium abundance can only increase monotonically, and dramatically, with time as the hydrogen layers are successively peeled off. In such a case, the correlation between He/H and T_e would actually be the inverse of the observed correlation (see Fig. 5). This suggests that mass loss is not the dominant process competing against settling in hot white dwarfs. We emphasize, however, that the role of stellar winds must be investigated quantitatively. The situation may be complicated by the fact that the mass-loss rate presumably decreases with decreasing effective temperature but also varies from one star to another (Bruhweiler and Kondo 1983). We can also imagine that *weak* winds can perturb the equilibrium abundances of levitating elements and, consequently, affect the EUV/soft X-ray emission of DA models along the cooling sequence. For example, such winds could empty the reservoir of a levitating heavy element. We can further imagine an intermediate case in which a wind is tapping the inner reservoir of helium but at a rate smaller than the rate of arrival of hydrogen migrating upward from the deep envelope! In that case, the sense of the correlation between He/H and T_e would be the same as that observed. It remains to be seen with detailed calculations how likely these various possibilities are.

A more attractive possibility at this time is the idea that ordinary diffusion, through the abundance gradient, is actually the main competitor of gravitational settling. Again referring to Figure 2, we can see that this is possible if our DA models are characterized by relatively thin H-rich layers (the curves would shift to the right). In such a case, the tail of the helium distribution (the linear part of the curve with a slope of 5) intercepts the photosphere at values of He/H much larger than those predicted by radiative levitation (which no longer plays an important role). This phenomenon of helium "pollution" is directly analogous to the carbon pollution problem discussed by Pelletier *et al.* (1986) in the context of cool, He-rich white dwarfs. Thus, in this model, hot DA stars can be interpreted as stratified objects with a H-rich outer layer that is so thin that some of the underlying helium is still visible (in a broader sense than in the optical window only). We develop further this idea in the remainder of this paper.

b) *Equilibrium between Ordinary Diffusion and Gravitational Settling*

The stratified models that we now consider are characterized uniquely by the competition between ordinary diffusion and gravitational settling. As mentioned previously, the helium abundance remains everywhere larger than that predicted by radiative levitation if the outer H-rich layer is sufficiently thin. Under such circumstances, the effects of radiative forces can be safely neglected and we take $g_r = 0$ from now on. If we assume that the H-He separation is complete,[5] the helium distribution can be directly obtained from equation (1). And indeed, the equilibrium condition ($w_{12} = 0$) can now be written,

$$\frac{\partial \ln c_2}{\partial r} = \left(\frac{A_1 Z_2 - A_2 Z_1}{Z_1 + \gamma Z_2}\right)\frac{m_p g}{kT} + \left(\frac{Z_2 - Z_1}{Z_1 + \gamma Z_2}\right)\frac{\partial \ln p_i}{\partial r}. \tag{11}$$

For an ideal, nondegenerate gas, it can be shown that,

$$\frac{\partial \ln p_i}{\partial r} = \frac{\partial \ln p}{\partial r} - \frac{(Z_2 - Z_1)}{(1 + Z_1) + \gamma(1 + Z_2)}\frac{1}{(1 + \gamma)}\frac{\partial \gamma}{\partial r}, \tag{12}$$

where p is the total pressure. In the derivation of this equation, the condition of charge neutrality [$p = p_1(1 + Z_1) + p_2(1 + Z_2)$] has been used, and it has been explicitly assumed that Z_1 and Z_2 do not vary with depth. From the condition of hydrostatic equilibrium, we have also

$$\frac{m_p g}{kT} = -\frac{\partial \ln p}{\partial r}\frac{[(1 + Z_1) + \gamma(1 + Z_2)]}{(A_1 + \gamma A_2)}. \tag{13}$$

By combining equations (11), (12), and (13), we obtain the following nonlinear differential equation for γ:

$$\frac{\partial \gamma}{\partial \ln p} = [E(\gamma)(A_2 Z_1 - A_1 Z_2) + D(\gamma)(Z_2 - Z_1)] \Big/ \left[\frac{C(\gamma)D(\gamma)}{\gamma B(\gamma)}\right] + \left[\frac{D(\gamma)(Z_2 - Z_1)^2}{B(\gamma)E(\gamma)}\right], \tag{14}$$

[5] We do restrict ourselves to equilibrium conditions in this section and do not study the approach to equilibrium which would require detailed time-dependent calculations.

where

$$B(\gamma) = 1 + \gamma \,, \tag{15}$$

$$C(\gamma) = Z_1 + \gamma Z_2 \,, \tag{16}$$

$$D(\gamma) = A_1 + \gamma A_2 \,, \tag{17}$$

and

$$E(\gamma) = (1 + Z_1) + \gamma(1 + Z_2) \,. \tag{18}$$

Equations (14)–(18) specify the equilibrium distribution of helium. For a given set A_1, A_2, Z_1, Z_2, the profile of element 2 (here helium) is uniquely determined on a logarithmic pressure scale. Note that the integration of equation (14) is of fundamental importance in any study of layered atmospheres.

The present derivation is analogous to that of Arcoragi and Fontaine (1980) and that of Jordan and Koester (1986), who show that an analytic solution of equation (14) is possible for certain special cases (e.g., a mixture of H II [$A_1 = 1$, $Z_1 = 1$] and He II [$A_2 = 4$, $Z_2 = 1$]). In general, however, only a numerical solution is possible. This is the case here, where over the range of effective temperature considered, hydrogen remains essentially totally ionized ($Z_1 = 1$), but the average charge of helium varies continuously from $Z_2 = 2$ to $Z_2 = 1$.

In practice, we use a model atmosphere to specify p_1, γ_1, and Z_2 (A_1, A_2, and Z_1 being known) at the photosphere. We assume that the average charge of helium is typified by its photospheric value (i.e., we neglect the possible variation of Z_2 with depth in a given model). We next integrate equation (14) inward until the value of γ becomes so large that only negligible traces of hydrogen are left further down. Hence, for a particular model atmosphere, we obtain the equilibrium helium distribution which is uniquely parametrized by the total mass of hydrogen in the outer layer M(H). We compute this quantity from the mass conservation equation,

$$\frac{dm(\mathrm{H})}{dr} = 4\pi r^2 \rho X(\mathrm{H}) \,, \tag{19}$$

where X(H) is the mass fraction of hydrogen, given by

$$X(\mathrm{H}) = \frac{1}{(1 + \gamma A_2/A_1)} \,. \tag{20}$$

By combining equation (19) with the equation of hydrostatic equilibrium, and neglecting the variations of radius and mass (a highly accurate approximation in the outermost layers of a white dwarf), we find the fractional mass of hydrogen

$$q(H) \equiv \frac{M(\mathrm{H})}{M} = \frac{4\pi G}{g^2} \int_{p_1}^{p} \frac{dp}{(1 + \gamma A_2/A_1)} \,, \tag{21}$$

where M is the total mass of the star, G is the gravitational constant, g is the (constant) gravity, and the other symbols have been defined previously. The integration is carried out to a large enough pressure so that the integrand (through an increasing value of γ) becomes practically negligible. We also use a simple expression to relate the fractional mass depth and the total pressure for a constant gravity atmosphere envelope,

$$q = \frac{4\pi G}{g^2} p \,. \tag{22}$$

Figure 6 illustrates some examples of helium distributions at equilibrium (*continuous curves*). It shows the relative number abundance of helium (called c_2 above) as a function of fractional mass depth in the outer layers of a stratified, 0.6 $M_\odot$ white dwarf model at $T_e = 60{,}000$ K. The gravity derived from the evolutionary tracks of Winget, Lamb, and Van Horn (1988) is $g = 7.29 \times 10^7$ cm s^{-2} ($\log g = 7.86$). With these parameters, simple gray atmosphere models indicate that the position of the Rosseland photosphere ($\bar{\tau} = 1$) is insensitive to helium abundance for He/H $\lesssim 10^{-2}$, and that relevant properties at that position are $\log p_1 = 6.57$, $\log q_1 = -15.27$, and $Z_2 = 1.88$. Using these values along with equation (14), we have computed three equilibrium distributions which differ by the surface value of He/H and, consequently, by the mass of the hydrogen layer. Curve 1 corresponds to a distribution with a photospheric (Rosseland) value $\gamma_1 = 10^{-2}$. The corresponding mass of the hydrogen layer is $\log q(\mathrm{H}) = -14.58$. This particular distribution can be taken as representative of DAO stars which are characterized by $T_e \sim 60{,}000$ K and He/H $\sim 10^{-2}$. Thus, these objects can be interpreted as stratified configurations with very thin hydrogen layers. Curves 2 and 3 illustrate the situation for somewhat thicker hydrogen layers. For a surface abundance $\gamma_1 = 10^{-3}$ (10^{-4}) the mass of the hydrogen layer is $\log q(\mathrm{H}) = -14.38$ (-14.19). These curves correspond to stratified configurations with hydrogen layers too thick to account for the DAO stars. It is interesting to point out how sensitive the photospheric helium abundance is to the thickness of the hydrogen layer: the surface value of He/H decreases by two orders of magnitude if q(H) increases by a factor ~ 2.5. This is due to the relatively large slope of the tail of the helium distribution. (See eqs. [6] and [7]), in conjunction with a Rosseland photosphere whose location is insensitive to the helium abundance.

It is straightforward to infer qualitatively that the *observable* He/H ratio can only decrease with decreasing effective temperature as is effectively observed. First, assume that H-He separation is complete in, say, the model appropriate for DAO stars (Fig. 6,

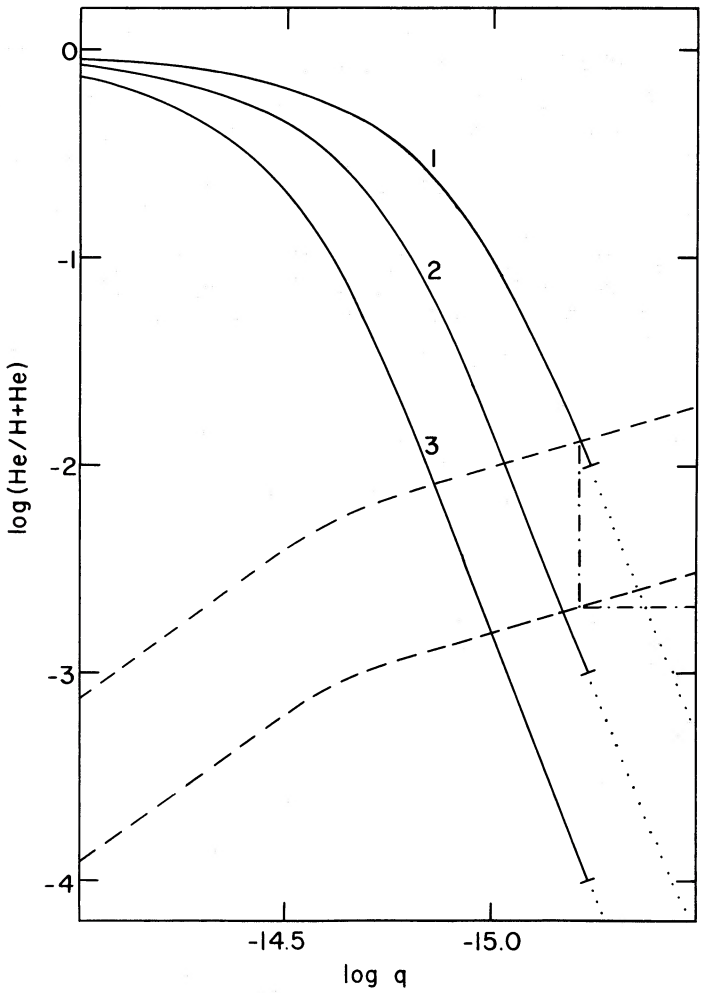

FIG. 6.—Equilibrium distributions of helium in stratified 0.6 $M_\odot$ DA models with T_e = 60,000 K. Curves labeled 1, 2, and 3 show equilibrium distributions for three cases which differ by the assumed thickness of the outer hydrogen layer. Dotted portion of each of the curves corresponds to the helium profile above the Rosseland photosphere. Upper (lower) dashed line corresponds to the relationship between depth and helium abundance at the X-ray photosphere for a layered (uniform) model atmosphere. Intersection of upper dashed line with an equilibrium distribution defines a consistent model (see text). Horizontal part of dash-dotted line is meant to illustrate the helium distribution of a homogeneous model.

curve 1). Furthermore, assume that the helium distribution is frozen in the star and does not change with time.[6] As cooling proceeds, the opacity of the atmospheric layers increases, and the location of the photosphere moves outward to smaller mass depths. As a result, less and less helium remains visible at the photosphere because the tail of the helium distribution must be projected to increasingly larger distances (the new position of the photosphere) from a frozen position. This results in a decreasing value of the observable He/H ratio with decreasing effective temperature.

Before we quantify the argument, however, some care must be taken in interpreting the observations. Contrary to the DAO stars, the helium abundances that are inferred from soft X-ray observations are *not* characteristic of the Rosseland photosphere, but bear the signature of physical conditions encountered near the X-ray photosphere, which is generally located deeper into the star. In other words, the soft X-ray observations probe a different stellar region than do the optical observations. As discussed in a previous section, the expected helium abundance at the Rosseland and at the X-ray photosphere is very roughly the same in presence of radiative levitation because the concentration gradient term is not very large as compared to other terms in the diffusion equation (see eq. [9]). However, in the present case where the effects of radiative levitation are negligible, the helium distribution is indeed very steep, and the abundance is a sensitive function of depth in the star. Thus, the observations must be carefully interpreted within the framework of the present model.

c) Helium Abundance at the X-Ray Photosphere

The first subtlety one encounters when dealing with helium abundances inferred from soft X-ray observations arises from the fact that the location of the X-ray photosphere is sensitive not only to the effective temperature but also to the helium abundance. This is not surprising, of course, because the soft X-ray flux is regulated by an opacity which is, in large part, controlled by the number of

[6] Strictly speaking, the conditions for equilibrium change with decreasing effective temperature (mostly through a change of Z_2 and g) so that the shape of the distribution is modified. However, this does not alter our present qualitative argument.

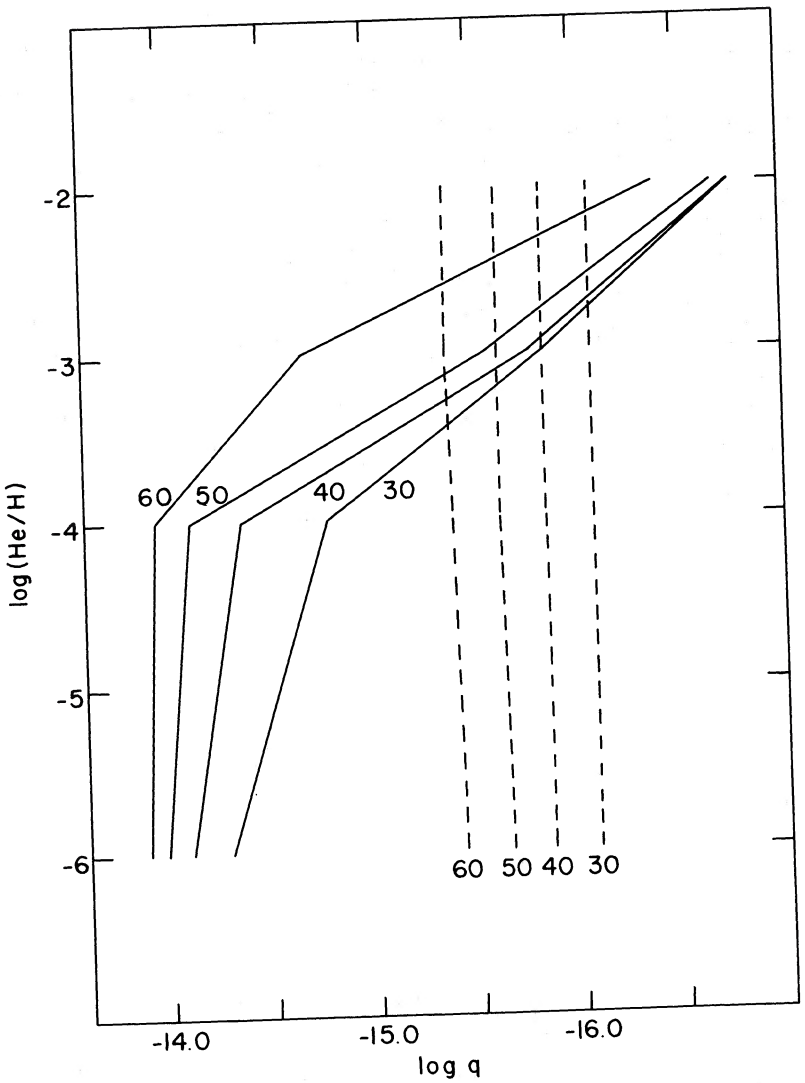

FIG. 7.—Relationship between depth (q) and helium abundance (He/H) at the photosphere of DA model atmospheres with uniform traces of helium and $\log g = 8.0$. Continuous curves correspond to the soft X-ray photosphere (~ 150 eV), and dashed curves to the Rosseland photosphere. Curves are labeled by the effective temperature of the models in units of 10^3 K.

helium absorbers. By contrast, the location of the Rosseland photosphere remains largely independent of the presence of helium traces because it is specified by an average opacity which reflects mostly the properties of the dominant atmospheric constituent, hydrogen.

The point is illustrated in Figure 7 where we have plotted, as a function of helium abundance, the location of both the Rosseland and X-ray photosphere for DA model atmospheres with $T_e(10^3\ \mathrm{K}) = 60$, 50, 40, and 30. We have used a subset of the grid of model atmospheres with homogeneous traces of helium described in Kahn *et al.* (1984). These models assume local thermodynamic equilibrium, plane-parallel geometry, include the blanketing of hydrogen lines, and are all at $\log g = 8.0$. We have transformed the photospheric column density provided by a given model atmosphere to the fractional mass appropriate for the $0.6\ M_\odot$ evolutionary model of the same effective temperature taken from the tracks of Winget, Lamb, and Van Horn (1988). This introduces a slight, and inconsequential inconsistency because the evolutionary models still show some residual contraction. Note also that the location of the Rosseland photosphere for the 60,000 K model is slightly different in Figure 6 than in Figure 7 because a gray atmosphere as opposed to a detailed model was used there. Finally, we have chosen to illustrate the behavior of the soft X-ray photosphere by picking the conditions appropriate to an energy ~ 150 eV ($\lambda = 85$ Å), which is representative of the spectral windows of both the *Einstein* and *EXOSAT* satellites.

As expected, the soft X-ray photosphere is generally located significantly deeper than the Rosseland photosphere. However, for values of the helium abundance as large as $\mathrm{He/H} = 10^{-2}$, the absorption of soft X-ray radiation becomes so large that the short-wavelength photons only escape from layers located above the Rosseland photosphere. Figure 7 illustrates clearly that the location of the soft X-ray photosphere (as opposed to that of the Rosseland photosphere) is indeed very sensitive to helium abundance. There is a hint in the figure that this sensitivity tends to disappear for very low helium abundances ($\mathrm{He/H} \lesssim 10^{-6}$). This, of course, is not surprising because, in the limit of negligible helium abundances, the location of the soft X-ray photosphere would be

determined by the minimal opacity offered by a pure hydrogen plasma. Figure 7 also shows that the effects of cooling are qualitatively the same for the two types of photosphere; i.e., as cooling proceeds, the photosphere moves outwards to smaller mass depths. Thus, for stratified models, not only will the observable He/H ratio at the Rosseland photosphere decrease with decreasing effective temperature (as pointed out previously), but so will the He/H ratio at the X-ray photosphere. However, the expected positive correlation between the observable He/H ratio and effective temperature is different in the case of soft X-ray observations than in the case of optical observations because, as we just discussed, the location of the soft X-ray photosphere depends on helium abundance. Detailed calculations show that the expected correlation between He/H and T_e must be *less* steep for the analyses based on short-wavelength observations. We note that, in practice, one can only hope to observe the correlation from soft X-ray observations because the sensitivity of optical or ultraviolet observations is limited to He/H $\gtrsim 10^{-3}$ for hot DA white dwarfs (Wesemael, Liebert, and Green 1984). The power of soft X-ray observations is to increase the sensitivity to helium abundance by some three orders of magnitude.

The second difficulty in interpreting soft X-ray observations is related to the fact that the helium abundance has been inferred from model atmospheres which assume uniform traces of helium in the vast majority of the analyses that have been carried out so far. Although, in the context of the proposed layered model, the helium distribution is far from being uniform, it is important to point out that we can still use with profit the available model atmospheres. And, indeed, in an optically thin medium, the monochromatic optical depth at a given point is essentially measured by the column density of absorbers above that point. We can therefore expect the soft X-ray flux in a hot DA white dwarf to be mostly determined by the overall opacity provided by absorbers above the soft X-ray photosphere, and not by the details of the distributions of absorbers—and, in particular, the distribution of helium—above the same level. Thus, we seek the equivalence in terms of column density between stratified models in diffusive equilibrium and models with uniform traces of helium.

To a good approximation, the soft X-ray opacity in the atmosphere of a hot, metal-free DA white dwarf is provided by bound-free transitions from the ground state of neutral hydrogen and from the ground state of He II, as well as scattering on free electrons. The monochromatic optical depth at the soft X-ray photosphere can then be written

$$\tau_\nu = 1 = \int_0^z \kappa_\nu \rho \, dz = \int_0^z (n(\text{He II})\sigma_\nu(\text{He II}) + n(\text{H I})\sigma_\nu(\text{H I}) + n_e \sigma_e) dz \, , \tag{23}$$

where n(He II)[n(H I)] is the number density of He II(H I) atoms (all assumed in the ground state), σ_ν(He II)[σ_ν(H I)] is the ground-state photoionization cross section for He II(H I) at frequency ν, n_e is the number density of free electrons, σ_e the Thompson scattering cross section, and z is the geometrical depth. As long as helium remains a *trace* element, the ionization balance as well as the distribution of hydrogen are essentially unaffected by the presence of helium, and the last two terms in equation (23) can be computed once and for all in a given model atmosphere. Under these circumstances, only the contribution of helium to the monochromatic optical depth (the first term in eq. [23]) may depend on the actual helium distribution. Using the equation of hydrostatic equilibrium, we rewrite this contribution for a stratified model in the form,

$$\tau_\nu(\text{He, stratified}) = \frac{\sigma_\nu(\text{He II})}{g} \int_{p_1}^{p} \frac{n(\text{He II})}{\rho} \, dp \, , \tag{24}$$

where p_1 is the pressure at some reference level in the upper atmosphere, p is the pressure at the soft X-ray photosphere, and, as before, g has been assumed constant. For all practical purposes, helium is only found in two ionization states (He II and He III) in the atmospheres of hot DA stars, so that there exists the simple relationship,

$$n_2 = \frac{n(\text{He II})}{(2 - Z_2)} \, , \qquad 1 \le Z_2 \le 2 \, , \tag{25}$$

where n_2 is the total number density of helium atoms and Z_2 is the average charge of helium as defined previously. If we neglect the variation of Z_2 with depth (as was done in the computation of the equilibrium distribution above), we obtain,

$$\tau_\nu(\text{He, stratified}) = \frac{\sigma_\nu(\text{He II})(2 - Z_2)}{g} \int_{p_1}^{p} \frac{n_2}{\rho} \, dp \, . \tag{26}$$

The integral that appears in equation (26) is a direct measure of the column density of helium atoms above the soft X-ray photosphere.

To proceed, we note that, for negligible helium abundances, the density is specified uniquely by hydrogen. This leads to

$$\frac{n_2}{\rho} = \frac{n_2}{m_p n_1} = \frac{\gamma}{m_p} \, . \tag{27}$$

Furthermore, in the tail of the helium distribution ($\gamma \ll 1$), equation (14) reduces to

$$\frac{\partial \gamma}{\partial \ln p} = \left[\frac{A_2}{A_1} (Z_1 + 1) - Z_2 - 1 \right] \gamma \equiv \beta \gamma \, . \tag{28}$$

This has a simple analytic solution given by

$$\gamma = \gamma_1 (p/p_1)^\beta \, , \tag{29}$$

where the index 1 refers to some reference level in the upper atmosphere. By combining equations (26), (27), and (29), we find

$$\tau_\nu(\text{He, stratified}) = \frac{\sigma_\nu(\text{He II})(2 - Z_2)}{m_p g} \frac{\gamma_1}{p_1^\beta} \int_{p_1}^{p} p^\beta dp \,. \tag{30}$$

If we further neglect p_1 in front of p (which is easily justified), we finally obtain

$$\tau_\nu(\text{He, stratified}) = \frac{\sigma_\nu(\text{He II})(2 - Z_2)}{m_p g} \frac{p\gamma}{\beta + 1} \,. \tag{31}$$

Similar considerations show that for a model with a *uniform* trace of helium $\gamma = \bar{\gamma}$ = constant,

$$\tau_\nu(\text{He, uniform}) = \frac{\sigma_\nu(\text{He II})(2 - Z_2)}{m_p g} p\bar{\gamma} \,. \tag{32}$$

At a given depth (i.e., at the same pressure p), the equality of equations (31) and (32) (which is equivalent to the equality of column densities) requires that

$$\gamma = (\beta + 1)\bar{\gamma} \,. \tag{33}$$

Hence, in the framework of the present model, the true abundance (γ) at the X-ray photosphere is simply $\beta + 1$ times the abundance ($\bar{\gamma}$) inferred by using models with a uniform distribution of helium. This very simple relationship has the distinct advantage that it allows us to use the available grid of uniform model atmospheres.

This is illustrated in Figure 6, where along with the three equilibrium distributions discussed previously, we have also plotted additional curves. The lower dashed curve gives the location of the soft X-ray photosphere in terms of log q as a function of helium abundance for uniform model atmospheres with T_e = 60,000 K and $M = 0.6\ M_\odot$. This curve is just a segment of what is illustrated in Figure 7. We recall that a value of $Z_2 = 1.88$ has been used in the computation of the equilibrium profiles at T_e = 60,000 K, and this corresponds to $(\beta + 1) = 6.12$ for this particular model. By multiplying the lower dashed curve by 6.12, we obtain the upper dashed curve which, according to previous arguments, gives the true relationship between depth and helium abundance at the X-ray photosphere for a layered model. *The intersection of this upper curve with a given equilibrium helium distribution profile uniquely defines the location and the helium abundance at the X-ray photosphere.* For example, Figure 6 shows that a 60,000 K, 0.6 $M_\odot$ layered model with log q(H) = −14.58 (curve 1) has a X-ray photosphere just slightly below the Rosseland photosphere (log q = −15.20) and that the helium abundance at that level is log (He/H) = −1.88. Note that the column density of helium above the X-ray photosphere is the *same* as that obtained from a model with a uniform trace of helium with $\bar{\gamma} = 10^{-2.67}$ (see the dash-dotted curve). Of course, this implies that a photospheric helium abundance He/H = $10^{-2.67}$ would be *inferred* if such a uniform model were to be used in the analysis. There is no inconsistency once one knows how to relate the two distributions. Figure 6 also shows that, for layered models with thicker hydrogen layers, the helium abundance at the X-ray photosphere would be log (He/H) = −2.00 (−2.10), and the X-ray photosphere would be located at log q = −15.03 (−14.86) for log q(H) = −14.38 (−14.19).

We have used similar principles to map extensively the domain of helium abundance-effective temperature characteristic of hot DA white dwarfs. We have sought to predict the helium abundance at the X-ray photosphere as a function of effective temperature for several layered models with given masses in the outer hydrogen layer. We have chosen to present the results in terms of the helium abundance that is inferred by using model atmospheres with uniform traces of helium because, once again, most of the analyses have been carried out with such models. It is to be understood that, in the remainder of this paper, we refer only to such abundance determinations.

The results of our computations are presented in Figure 8 which also summarizes the essential results of this paper. First, we have reported in the figure the data of Table 2; this illustrates the observed correlation between the photospheric abundance of helium and effective temperature. For consistency, we have transformed the helium abundances observed at the Rosseland photosphere of DAO objects into abundances that would be inferred at the X-ray photosphere (*open circles*). For example, we find from above that a value of He/H = 10^{-2} at the Rosseland photosphere in a 0.6 $M_\odot$, 60,000 K DAO model corresponds to He/H = $10^{-2.7}$ at the X-ray photosphere. The continuous curves correspond to the predicted helium abundance at the X-ray photosphere as a function of effective temperature for layered models in which an equilibrium between gravitational settling and ordinary diffusion has been reached. The various curves are labeled by the fractional mass of the outer hydrogen layer; log q(H) = −15.0, −14.5, −14.0, −13.5, and −13.0, from top to bottom, respectively. They all refer to sequences of models with parameters taken from the 0.6 $M_\odot$ evolutionary track of Winget, Lamb, and Van Horn (1988). The theoretical curves all show a positive correlation between helium abundance and effective temperature. As explained previously, this is the result of a simple opacity effect which pushes the soft X-ray photosphere outward, to regions of smaller helium abundance, as cooling proceeds.

A comparison of the theoretical predictions with the observations shows that the latter can naturally be explained within the framework of layered models. In particular, the observed positive correlation between He/H and T_e appear to be simply related to a cooling effect. We note also that the hydrogen layers in hot DA white dwarfs appear to be remarkably thin. An equally remarkable result is the fact that the observed correlation between He/H and T_e is *steeper* than that obtained for an evolving model in which the mass of the outer layer of hydrogen is kept constant. Figure 8 suggests that the observations can be accounted for if, on average, the mass and thickness of the hydrogen layer increase with decreasing effective temperature. For example, a value He/H = $10^{-2.5}$ at the soft X-ray photosphere of a typical DAO star is the natural product of helium pollution through a rather thin hydrogen layer containing only a fractional mass log q(H) ≈ −14.7 ($M = 0.6\ M_\odot$ and T_e = 60,000 K assumed). Likewise, an observed photo-

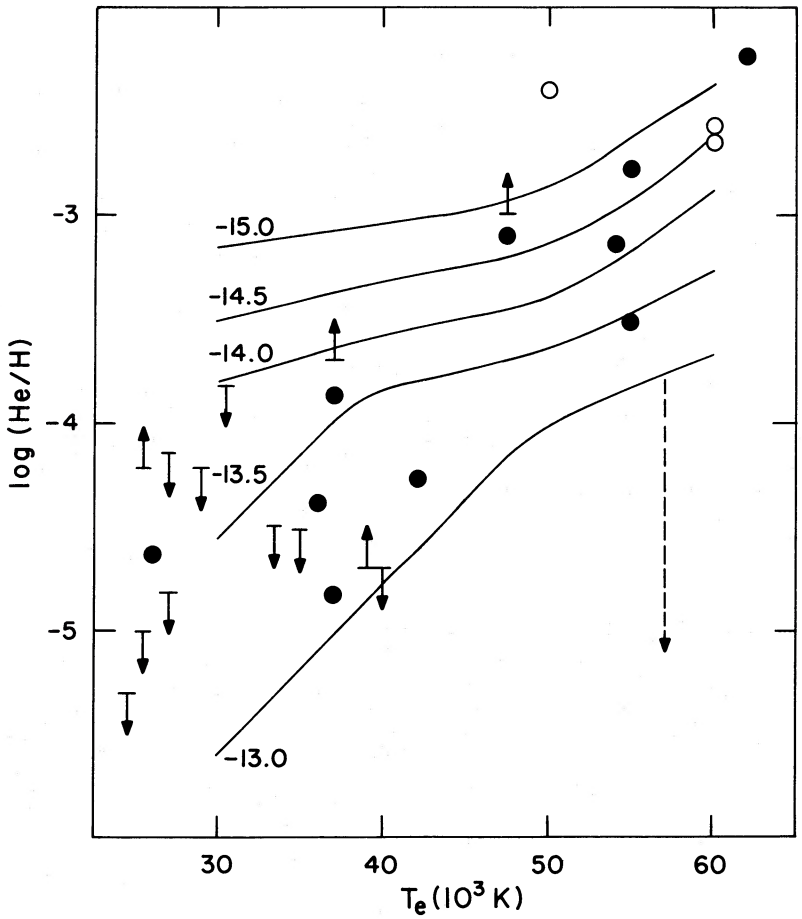

FIG. 8.—Predicted correlation between helium abundance *at the soft X-ray photosphere* (85 Å) of homogeneous model atmospheres and effective temperature. Observational data (*arrows, filled and open circles*) are reported from Fig. 5. Continuous lines correspond to the expected abundance for models with various values for the mass of the hydrogen layer, parametrized here by log q(H).

spheric value He/H $\sim 10^{-5}$ (more typical of $\sim$30,000 K DA stars) can be explained with a model which has log q(H) ≈ -13.3. *Thus, Figure 8 strongly suggests that H-He separation still goes on in cooling DA white dwarfs between T_e = 60,000 K and T_e = 30,000 K.*

The observational scatter shown in the figure must certainly be due in part to variations in log q(H) from one object to another at a given effective temperature and in part to observational uncertainties related to the determination of atmospheric parameters. However, the influence of gravity is likewise quite important in this diagram. In particular, the case of HZ 43 (which weakens somewhat the observed correlation between He/H and T_e) can be explained naturally here: the one identified characteristic which distinguishes HZ 43 from the other hot ($T_e \gtrsim$ 50,000 K) DA white dwarfs is its suggested large gravity (see Table 2). More massive white dwarfs are characterized by denser, less transparent outer layers (see Fontaine and Van Horn 1976), and one might expect that the ability to detect photospheric traces of helium at a given level is correspondingly reduced. This expectation is, in fact, borne out by detailed computations which make use of atmosphere models at log g = 8.5, with various uniform traces of helium. If we identify HZ 43 as a massive white dwarf with T_e = 57,500 K and log g = 8.5 (this corresponds to 0.9 $M_\odot$ on the Chandrasekhar tracks for material with μ_e = 2), we find that the He/H ratio at the soft X-ray photosphere is less than $10^{-5.22}$ if the fractional mass of hydrogen is larger than log q(H) = −13.55. Thus, HZ 43 does not *have* to be an unusual DA white dwarf in the sense that it must have a substantially more massive outer hydrogen layer than more typical objects (which would be another way of explaining the location of HZ 43 in Fig. 8). The present result shows that the ability to detect traces of helium in a hot DA white dwarf through soft X-ray observations is rather sensitive to gravity. This should be taken into account when analyzing observations of individual objects. Likewise, the present result suggests that a significant part of the observational scatter shown in Figure 8 could be related to small gravity differences from one object to another.

V. DISCUSSION

We have found that a likely possibility for explaining the presence of photospheric traces of helium in hot DA white dwarfs is the idea that these objects have a stratified configuration (through an equilibrium between gravitational settling and ordinary diffusion) with an outer H-rich layer that is so thin that small amounts of helium remain visible, particularly at short wavelengths which probe generally deeper into such stars. This idea is not new and has been invoked by several authors (see, in particular, Jordan and Koester 1986, and references therein). What is new, however, is perhaps the realization that thin hydrogen layers are more the rule

than the exception in hot DA white dwarfs, and that alternate possibilities (e.g., radiative levitation, accretion, winds) are not very attractive if not downright unviable. And, indeed, the importance of the layered configuration model for hot DA white dwarfs is underscored by the fact that the current sample of objects which have been analyzed is representative of the hot DA population as a *whole*. There has been no special selection criteria used in choosing the 24 objects which have been observed with the *Einstein* or *EXOSAT* satellites; these targets are simply the bright (i.e., nearby) hot DA stars in the solar neighborhood. *Thus, if the layered atmosphere model proves correct, most, if not all, hot DA white dwarfs must have very thin outer hydrogen layers.*

We have mentioned previously that thin layers have been invoked in a number of analyses of individual hot DA white dwarfs. As an example, we comment briefly on the recent *EXOSAT* observation of Feige 24 by Paerels *et al.* (1986*b*). These authors have encountered great difficulties in trying to explain the EUV spectrum of that star in terms of homogeneous model atmospheres. They suggest instead that the atmosphere of Feige 24 might be layered. Although this discussion is in no way a substitute for a forthcoming detailed analysis of the *EXOSAT* data, we find it indeed very tempting to identify Feige 24 with one of the stratified models published by Jordan and Koester (1986). For example, model 8 shown on Figure 6*d* of that paper (model with $\log g = 8.0$, $T_e = 60{,}000$ K, and referred to as a "thick" model) appears to have enough EUV flux and yet enough opacity to be relevant to the Feige 24 observations. The model corresponds to a stratified object with a total mass of hydrogen $q(\mathrm{H}) \sim 10^{-14.1}$. This layer of hydrogen is sufficiently thick that the optical spectrum is identical to that of a pure hydrogen atmosphere. At the same time, it is sufficiently thin that some helium pollutes the EUV photosphere from below and absorbs some of the short-wavelength flux. It is interesting to point out that the value of $q(\mathrm{H})$ suggested for Feige 24 is remarkably close to similar values suggested here for the very hot DA white dwarfs. Although the presence of metals complicates the picture, further analyses of the Feige 24 data along the lines of Jordan and Koester (1986) seem very promising.

The present suggestion that hot DA white dwarfs have very thin H-rich layers is also consistent with (and gives additional support to) the model recently put forward by Fontaine *et al.* (1988) which suggests a common origin for the white dwarfs of various spectral types. In this model, it is envisioned that the He-rich PG 1159–type stars are the hot progenitors of the majority of the white dwarfs. It is assumed that very small traces of hydrogen are left over in the envelopes of these very hot objects. As a function of time, hydrogen migrates upward and accumulates at the surface until the star appears as a DA when a full atmosphere of hydrogen has been built up. This turnover in the compositional character of the star's atmosphere occurs at effective temperatures significantly lower than those characteristic of the PG 1159–type objects. In addition, the effective temperature of the turnover depends on the total amount of hydrogen initially hidden in the progenitor; those PG 1159 stars that have more hydrogen overall turn into DA stars earlier. The model provides a natural explanation for the lack of very hot DA stars, the changing ratio of DA to non–DA white dwarfs as a function of cooling, and the gap in the distribution of He-rich white dwarfs in the range $30{,}000 \lesssim T_e \lesssim 45{,}000$ K (see also Liebert, Fontaine, and Wesemael 1987; Fontaine and Wesemael 1987). It also implies that most DA white dwarfs are born and evolve with much thinner H-rich layers than predicted by standard evolution theory. Preliminary calculations show that the expected hydrogen layer mass in a DA star with $T_e = 60{,}000$ K is remarkably similar to the mass inferred here for DAO objects. The thickness of the H layer may substantially increase, however, because separation of hydrogen and helium may still go on until the star has cooled to $T_e \sim 30{,}000$ K, depending on the initial amount of hydrogen. This provides, in a natural way, a spectrum of possible masses for the external H-rich layer. At the same time, this also provides an attractive explanation for the increase of the mass of the hydrogen layer (observed in Fig. 8) as a function of decreasing effective temperature. More detailed calculations of H-He separation in white dwarfs are in order at this point.

It is interesting to examine some consequences of the suggestion that hot DA white dwarfs have very thin outer hydrogen layers. Perhaps the most provocative one is the resulting conflict with standard evolution theory which predicts that DA white dwarfs should be born with massive [$\log q(\mathrm{H}) \approx -4.0$] hydrogen layers (see Iben and Tutukov 1984; Iben and MacDonald 1985; Koester and Schönberner 1986). It may be recalled that evidence in favor of thin hydrogen layers in *cool* DA white dwarfs has been around for some time. A first argument is based on the statistics of H- and He-dominated white dwarf atmospheres below $T_e \sim 10{,}000$ K. Convective mixing of thin [$\log q(\mathrm{H}) \lesssim -8.0$] hydrogen layers with an underlying helium convection zone is the most likely (and most often invoked) mechanism to account for the turnover of white dwarf statistics in favor of He-dominated atmospheres at low effective temperatures (Koester 1976; Vauclair and Reisse 1977; Sion 1984, and references therein). An independent piece of evidence comes from the pulsational studies of Winget *et al.* (1982) and Winget and Fontaine (1982) which require that ZZ Ceti star models must have thin [$\log q(\mathrm{H}) \lesssim -7.0$] hydrogen layers if the theoretical blue edge of the instability strip is to be identified with the observed blue edge at $T_e \approx 13{,}000$ K. As most of the DA white dwarfs are believed to become ZZ Ceti pulsators as they enter the instability strip (Fontaine *et al.* 1982), this means that, if DA white dwarfs begin their cooling phase with massive hydrogen layers, they must have gotten rid of most of their hydrogen by the time they have cooled to the ZZ Ceti effective temperature range. Similarly, DA white dwarfs produced by standard evolution theory must also manage to get rid of most of their hydrogen if they are to mix at low effective temperatures.

Prompted by this conflict, Michaud and Fontaine (1984) proposed that diffusion-induced hydrogen burning could possibly reduce significantly the mass of the outer layer of hydrogen of a DA white dwarf during its evolution. However, Iben and MacDonald (1985) used detailed evolutionary calculations to demonstrate that the efficiency of this new mechanism was insufficient to reconcile standard evolution theory with the evidence that is available at the cool end of the DA sequence. They proposed—but did not pursue actual calculations—that mass loss could be the key mechanism. Since there is only evidence for accretion in cooler white dwarfs, and since strong winds conflict with the soft X-ray observations of hot DA white dwarfs (see above), the contradiction between the predictions of standard evolution theory and our knowledge of white dwarfs has remained. The present results make this conflict even more severe than before because they suggest that DA white dwarfs *are* born with only very thin hydrogen layers. By contrast, the same results are fully consistent with what we know about ZZ Ceti stars and cooler DA white dwarfs.

One final observation is that the masses that we find for the hydrogen layers in hot DA white dwarfs (see Fig. 8) are so small that nuclear burning must be totally negligible in isolated white dwarfs. Also, these masses are so small that interesting limits can be put

on possible winds in these objects. If, for example, a value log $q(\mathrm{H}) \approx -13.13$ is typical of a 30,000 K stratified DA white dwarf (see above), we find that mass loss cannot operate at a rate much larger than $\sim 10^{-21}\ M_{\odot}\ \mathrm{yr}^{-1}$ in such an object. Otherwise, the thin hydrogen layer would evaporate in less than a cooling time. Note that such a weak wind could still play havoc with the abundances of heavy elements supported by radiative levitation and its effects deserve to be studied. However, weak winds do not perturb significantly the overall evolution of white dwarfs.

To summarize, we find that ordinary diffusion can efficiently compete against gravitational settling in the atmospheres and envelopes of hot DA white dwarfs. The consequences of the combined effects of these two processes appear to be most attractive in terms of explaining the observations discussed here. By contrast, we also find that radiative levitation of helium cannot, by itself, account for the same observations. However, the cumulative effects of several levitating elements in terms of providing enough soft X-ray opacity remain to be investigated. We do not favor accretion of absorbers from the interstellar medium on the grounds that the required rates appear to be unacceptably large. Likewise, mass loss is not favored, although its more subtle effects must be studied in detail. If ordinary diffusion and gravitational settling are indeed the dominant mechanisms, then hot DA white dwarfs must have very thin hydrogen layers. This is in strong contradiction with the predictions of standard evolution theory. At the same time, however, the same suggestion adds to what may be considered mounting evidence in favor of relatively thin layers of hydrogen and helium in white dwarf stars. We note also that thin layers, of helium this time, are also required to understand the carbon pollution observed in the atmospheres of DC and DQ white dwarfs (Fontaine, *et al.* 1984; Pelletier *et al.* 1986).

We wish to thank G. Michaud for pertinent discussions. We are also thankful to the Centre de Calcul of the Université de Montréal for generous allotments of computer time. Partial financial support for this work has been provided by NSERC Canada and the fund FCAR (Québec).

REFERENCES

Alcock, C., and Illarionov, A. 1980, *Ap. J.*, **235**, 534.
Alecian, G., and Grappin, R. 1984, *Astr. Ap.*, **140**, 159.
Arcoragi, J.-P., and Fontaine, G. 1980, *Ap. J.*, **242**, 1208.
Bruhweiler, F. D., and Kondo, Y. 1983, *Ap. J.*, **269**, 657.
Chapman, S., and Cowling, T. G. 1970, *The Mathematical Theory of Nonuniform Gases* (3d ed.; Cambridge: Cambridge University Press).
Chayer, P. 1987, M.Sc. thesis, Université de Montréal.
Chayer, P., Fontaine, G., Wesemael, F., and Michaud, G. 1987, in *IAU Colloquium 95, The Second Conference on Faint Blue Stars*, ed. A. G. D. Philip, D. S. Hayes, and J. Liebert (Schenectady: Davis), p. 653.
Fontaine, G., Graboske, H. C., Jr., and Van Horn, H. M. 1977, , *Ap. J. Suppl.*, **35**, 293.
Fontaine, G., Kawaler, S. D., Pelletier, C., Wesemael, F., and Winget, D. E. 1988, in preparation.
Fontaine, G., McGraw, J. T., Dearborn, D. S. P., Gustafson, J., and Lacombe, P. 1982, *Ap. J.*, **258**, 651.
Fontaine, G., and Michaud, G. 1979, *Ap. J.*, **231**, 826.
Fontaine, G., and Van Horn, H. M. 1976, *Ap. J. Suppl.*, **31**, 467.
Fontaine, G., Villeneuve, G., Wesemael, F., and Wegner, G. 1984, *Ap. J. (Letters)*, **277**, L51.
Fontaine, G., and Wesemael, F. 1987, in *IAU Colloquium 95, The Second Conference on Faint Blue Stars*, ed. A. G. D. Philip, D. S. Hayes, and J. Liebert (Schenectady: Davis), p. 319.
Fontaine, G., Wesemael, F., Vennes, S., and Pelletier, C. 1987, *Bull. AAS*, **19**, 1115.
Heise, J. 1985, *Space Sci. Rev.*, **40**, 79.
Heise, J., Paerels, F. B. S., Bleeker, J. A. M., and Brikman, A. C. 1988, preprint.
Henry, R. B. C., Shipman, H. L., and Wesemael, F. 1985, *Ap. J. Suppl.*, **57**, 145.
Holberg, J. B. 1987*a*, in *IAU Colloquium 95, The Second Conference on Faint Blue Stars*, ed. A. G. D. Philip, D. S. Hayes, and J. Liebert (Schenectady: Davis), p. 285.
———. 1987*b*, private communication.
Holberg, J. B., Sion, E. M., and Vauclair, G. 1987, *Bull. AAS.*, **19**, 1041.
Holberg, J. B., Wesemael, F., and Basile, J. 1986, *Ap. J.*, **306**, 629.
Holberg, J. B., Wesemael, F., and Hubený, I. 1984, *Ap. J.*, **280**, 679.
Huebner, W. J. 1980, private communication.
Iben, I., Jr., and MacDonald, J. 1985, *Ap. J.*, **296**, 540.
Iben, I., Jr., and Tutukov, A. V. 1984, *Ap. J.*, **282**, 615.
Jensen, K. A., Swank, J. H., Petre, R., Guinan, E. F., Sion, E. M., and Shipman, H. L. 1986, *Ap. J. (Letters)*, **309**, L27.
Jordan, S., and Koester, D. 1986, *Astr. Ap. Suppl.*, **65**, 367.
Jordan, S., Koester, D., Wulf-Mathies, C., and Brunner, H. 1987, *Astr. Ap.*, **185**, 253.
Kahn, S. M., Wesemael, F., Liebert, J., Raymond, J. C., Steiner, J. E., and Shipman, H. L. 1984, *Ap. J.*, **278**, 255.
Koester, D. 1976, *Astr. Ap.*, **52**, 415.
Koester, D., Liebert, J., and Hege, E. K. 1979, *Astr. Ap.*, **71**, 163.
Koester, D., and Schönberner, D. 1986, *Astr. Ap.*, **154**, 125.
Liebert, J., Fontaine, G., and Wesemael, F. 1987, *Mem. Soc. Astr. Italiane*, **58**, 17.
Margon, B., Bolte, M., and Anderson, S. F. 1987, *A.J.*, **93**, 1229.
Mendez, R. H., Kudritzki, R. P., Gruschinske, J., and Simon, K. P. 1981, *Astr. Ap.*, **101**, 323.
Michaud, G. 1982, private communication.
Michaud, G., and Fontaine, G. 1984, *Ap. J.*, **283**, 787.
Michaud, G., Montmerle, T., Cox, A. N., Magee, N. H., Hodson, S. W., and Martel, A. 1979, *Ap. J.*, **234**, 206.
Muchmore, D. O. 1984, *Ap. J.*, **278**, 679.
Paerels, F. B. S., Bleeker, J. A. M., Brinkman, A. C., Gronenschild, E. B. H. M., and Heise, J. 1986*a*, *Ap. J.*, **308**, 190.
Paerels, F. B. S., Bleeker, J. A. M., Brinkman, A. C., and Heise, J. 1986*b*, *Ap. J. (Letters)*, **309**, L33.
———. 1988, preprint.
Paerels, F. B. S., Heise, J., Kahn, S. M., and Rogers, R. D. 1987, *Ap. J.*, **322**, 315.
Paerels, F. B. S., and Heise, J. 1988, preprint.
Paquette, C., Pelletier, C., Fontaine, G., and Michaud, G. 1986*a*, *Ap. J. Suppl.*, **61**, 197.
———. 1986*b*, *Ap. J. Suppl.*, **61**, 177.
Pelletier, C. 1986, Ph.D. thesis, Université de Montréal.
Pelletier, C., Fontaine, G., Wesemael, F., Michaud, G., and Wegner, G. 1986, *Ap. J.*, **307**, 242.
Petre, R., and Shipman, H. L. 1987, *Bull. AAS*, **19**, 1041.
Petre, R., Shipman, H. L., and Canizares, C. R. 1986, *Ap. J.*, **304**, 356.
Pravdo, S. H., Marshall, F. E., White, N. E., and Giommi, P. 1986, *Ap. J.*, **300**, 819.
Schatzman, E. 1958, *White Dwarfs* (Amsterdam: North Holland).
Shipman, H. L. 1976, *Ap. J. (Letters)*, **206**, L67.
Sion, E. M. 1984, *Ap. J.*, **282**, 612.
Vauclair, G., and Reisse, C. 1977, *Astr. Ap.*, **61**, 415.
Vauclair, G., Vauclair, S., and Greenstein, J. L. 1979, *Astr. Ap.*, **80**, 79.
Vennes, S. 1985, M.Sc. thesis, Université de Montréal.
Vennes, S., Pelletier, C., Fontaine, G., and Wesemael, F. 1987, in *IAU Colloquium 95, The Second Conference on Faint Blue Stars*, ed. A. G. D. Philip, D. S. Hayes, and J. Liebert (Schenectady: Davis), p. 665.
Wesemael, F. 1979, *Astr. Ap.*, **85**, 208.
Wesemael, F., Green, R. F., and Liebert, J. 1985, *Ap. J. Suppl.*, **58**, 379.
Wesemael, F., Henry, R. B. C., and Shipman, H. L. 1984, *Ap. J.*, **287**, 868.
Wesemael, F., Liebert, J., and Green, R. F. 1984, *Pub. A.S.P.*, **96**, 981.
Winget, D. E., and Fontaine, G. 1982, in *Pulsations in Classical and Cataclysmic Variables*, ed. J. P. Cox and C. . J. Hansen (Boulder: University of Colorado Press), p. 142.
Winget, D. E., Lamb, D. Q., and Van Horn, H. M. 1988, in preparation.
Winget, D. E., Van Horn, H. M., Tassoul, M., Hansen, C. J., Fontaine, G., and Carroll, B. W. 1982, *Ap. J. (Letters)*, **253**, L29.

G. Fontaine, C. Pelletier, S. Vennes, and F. Wesemael: Département de Physique, Université de Montréal, C.P. 6128, Succ. A, Montréal, Québec, Canada H3C 3J7